Comparison of eccentric waveform models on a HTC cluster

Numerical Analysis of Mismatch Between Eccentric Gravitational Waves

Balázs Kacskovics

Relation to HEP

My Place in the Local Spacetime Manifold

- Looking for small effect
- The high amount of energy radiated

GW150914: FACTSHEET

BACKGROUND IMAGES: TIME-FREQUENCY TRACE (TOP) AND TIME-SERIES (BOTTOM) IN THE TWO LIGO DETECTORS; SIMULATION OF BLACK HOLE HORIZONS (MIDDLE-TOP), BEST FIT WAVEFORM (MIDDLE-BOTTOM)

first direct detection of gravitational waves (GW) and first direct observation of a black hole binary

observed by	LIGO L1, H1
source type	black hole (BH) binary
date	14 Sept 2015
time	09:50:45 UTC
likely distance	0.75 to 1.9 Gly 230 to 570 Mpc
redshift	0.054 to 0.136
signal-to-noise ratio	24
false alarm prob.	< 1 in 5 million
false alarm rate	< 1 in 200,000 yr
Source Masses	$M_\odot$
total mass	60 to 70
primary BH	32 to 41
secondary BH	25 to 33
remnant BH	58 to 67
mass ratio	0.6 to 1
primary BH spin	< 0.7
secondary BH spin	< 0.9
remnant BH spin	0.57 to 0.72
signal arrival time delay	arrived in L1 7 ms before H1
likely sky position	Southern Hemisphere
likely orientation	face-on/off
resolved to	~600 sq. deg.

duration from 30 Hz	~ 200 ms
# cycles from 30 Hz	~10
peak GW strain	1×10^{-21}
peak displacement of interferometers arms	±0.002 fm
frequency/wavelength at peak GW strain	150 Hz, 2000 km
peak speed of BHs	~ 0.6 c
peak GW luminosity	3.6×10^{56} erg s^{-1}
radiated GW energy	2.5-3.5 $M_\odot$
remnant ringdown freq.	~ 250 Hz
remnant damping time	~ 4 ms
remnant size, area	180 km, 3.5×10^5 km^2
consistent with general relativity?	passes all tests performed
graviton mass bound	$< 1.2 \times 10^{-22}$ eV
coalescence rate of binary black holes	2 to 400 Gpc^{-3} yr^{-1}
online trigger latency	~ 3 min
# offline analysis pipelines	5
CPU hours consumed	~ 50 million (=20,000 PCs run for 100 days)
papers on Feb 11, 2016	13
# researchers	~1000, 80 institutions in 15 countries

Detector noise introduces errors in measurement. Parameter ranges correspond to 90% credible bounds.

Acronyms: L1=LIGO Livingston, H1=LIGO Hanford; Gly=giga lightyear=9.46×10^{12} km; Mpc=mega parsec=3.2 million lightyear, Gpc=10^3 Mpc, fm=femtometer=10^{-15} m, $M_\odot$=1 solar mass=2×10^{30} kg

“I am your father’s, brother’s, nephew’s, cousin’s, former roommate. - What does that make us? - Absolutely nothing...„

Spaceballs — 1987

Motivation

PRL 114, 141101 (2015)

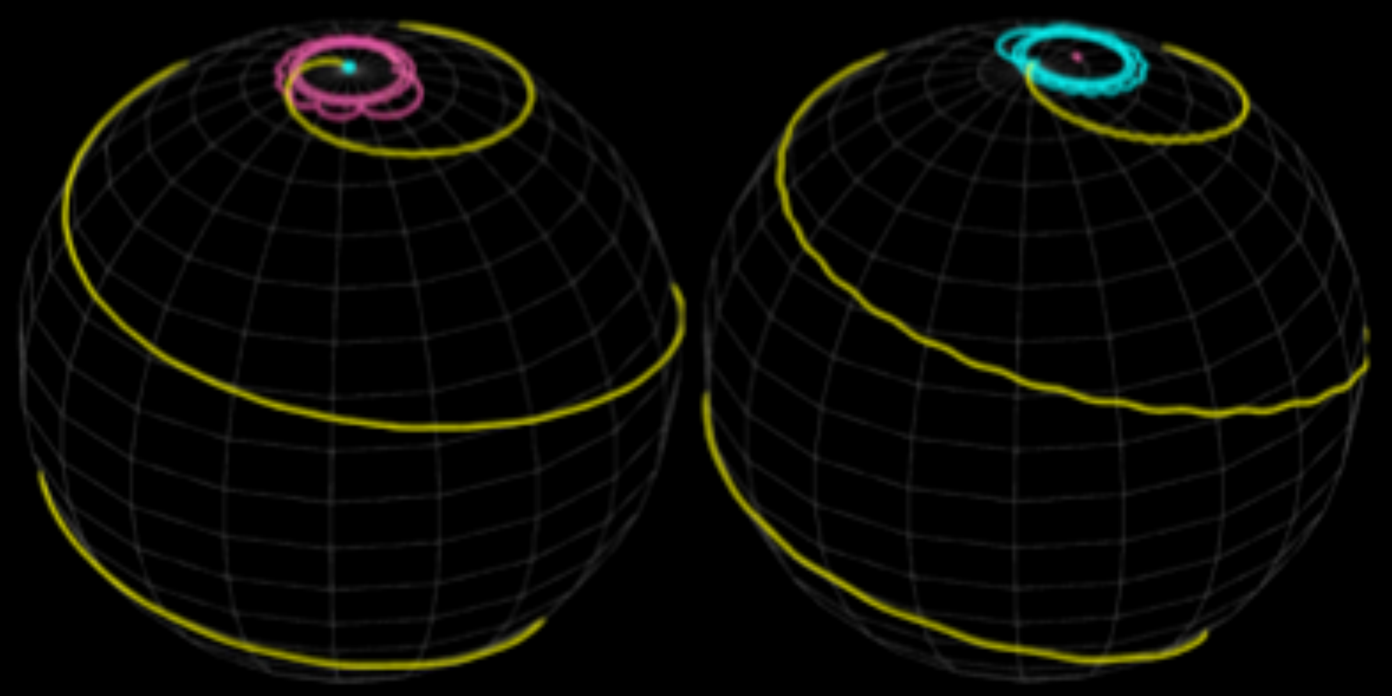

ApJ 883, 149 (2019)

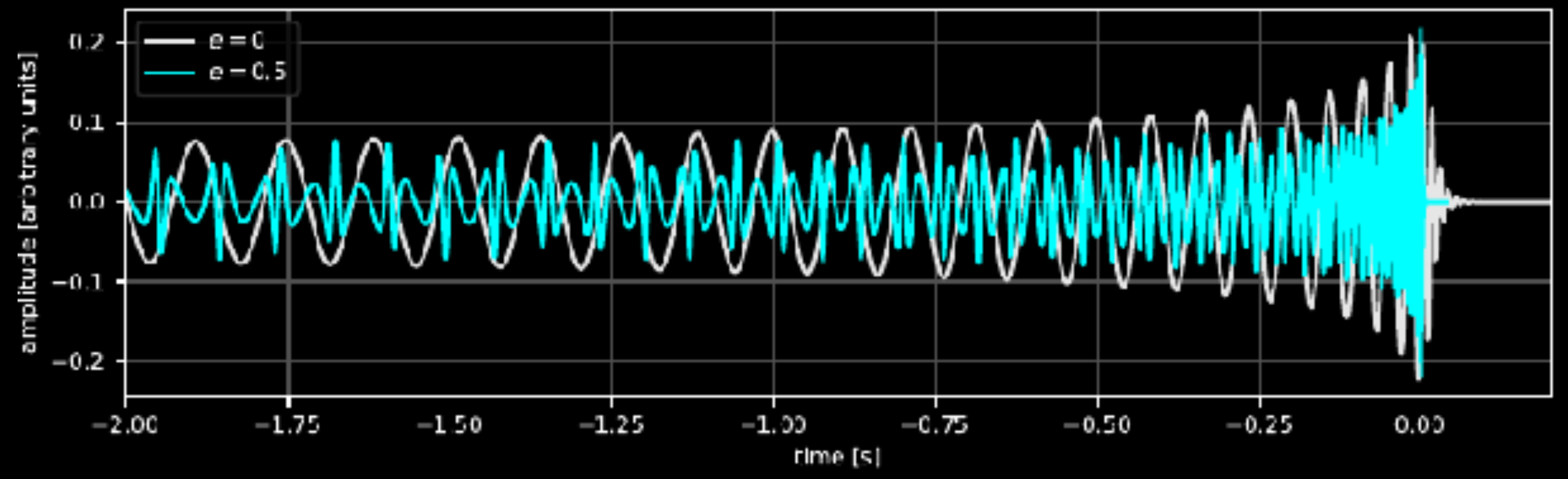

soundsofspacetime.org

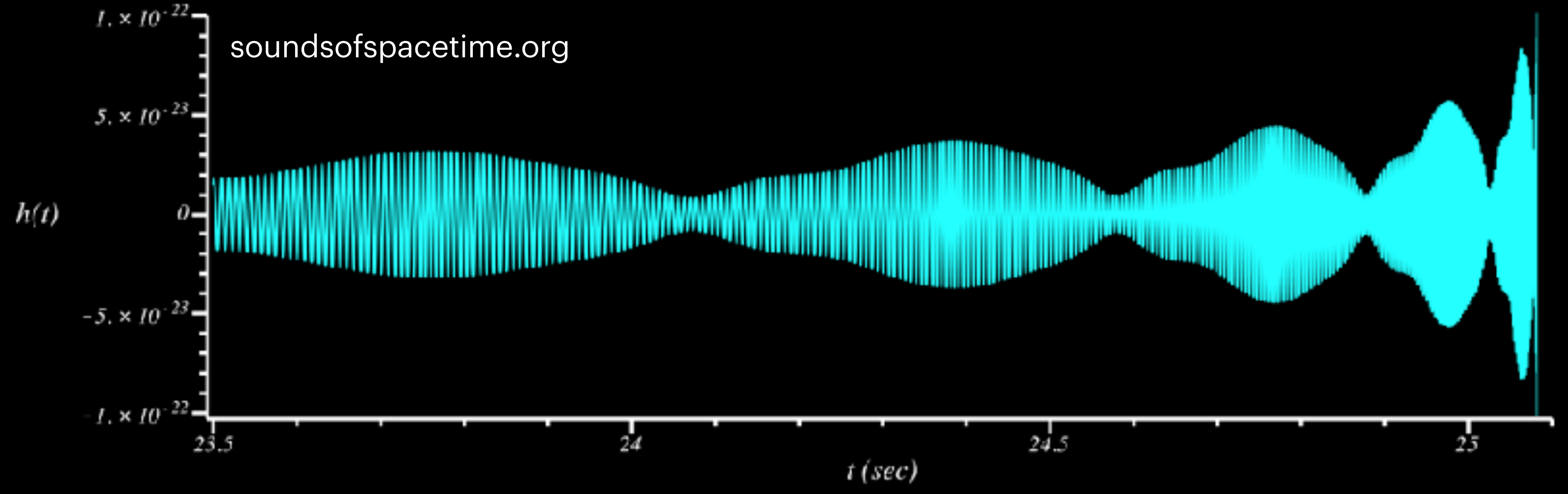

PRL 114, 141101 (2015)

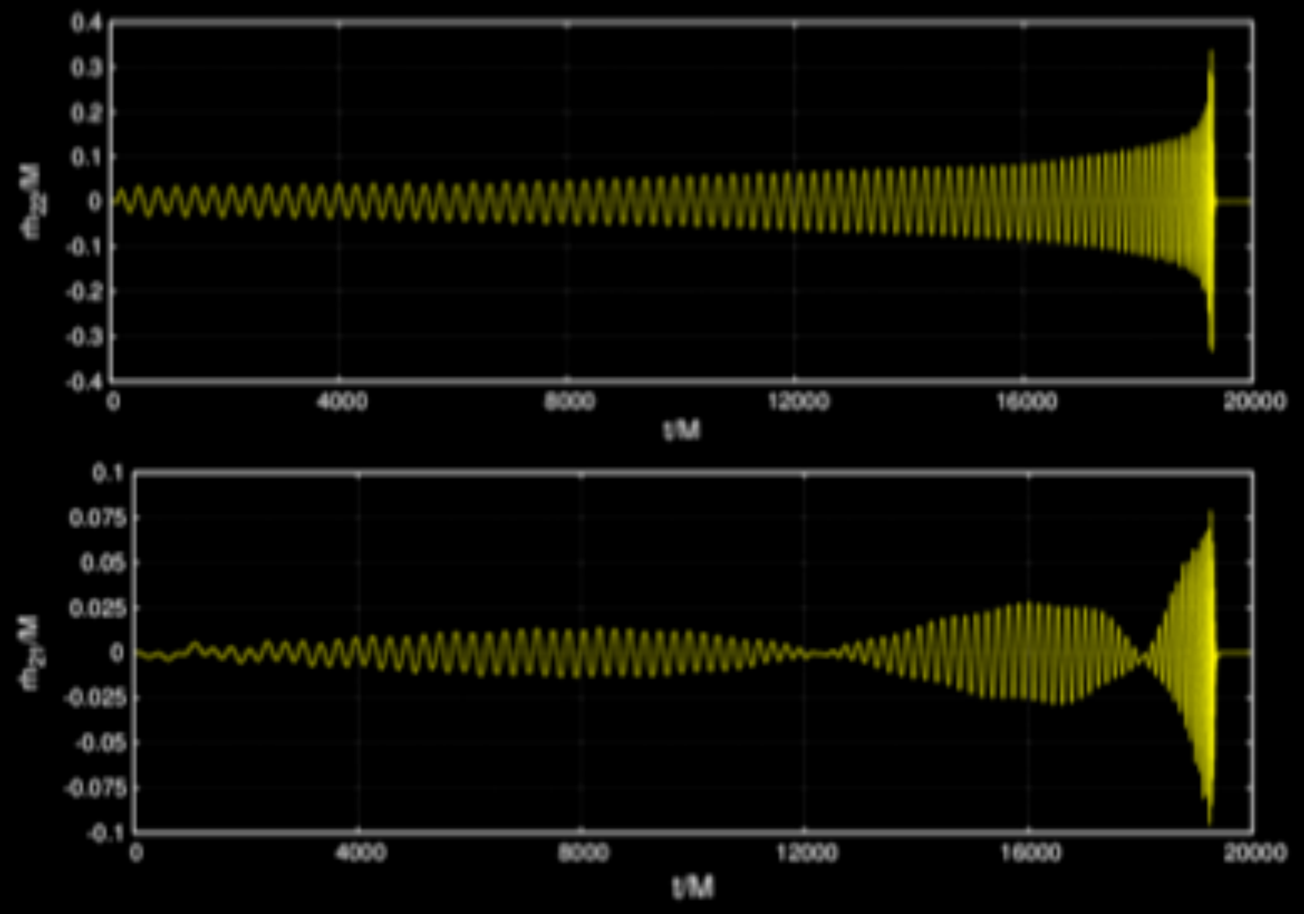

Class. Quantum Grav. 39, 095007 (2022)

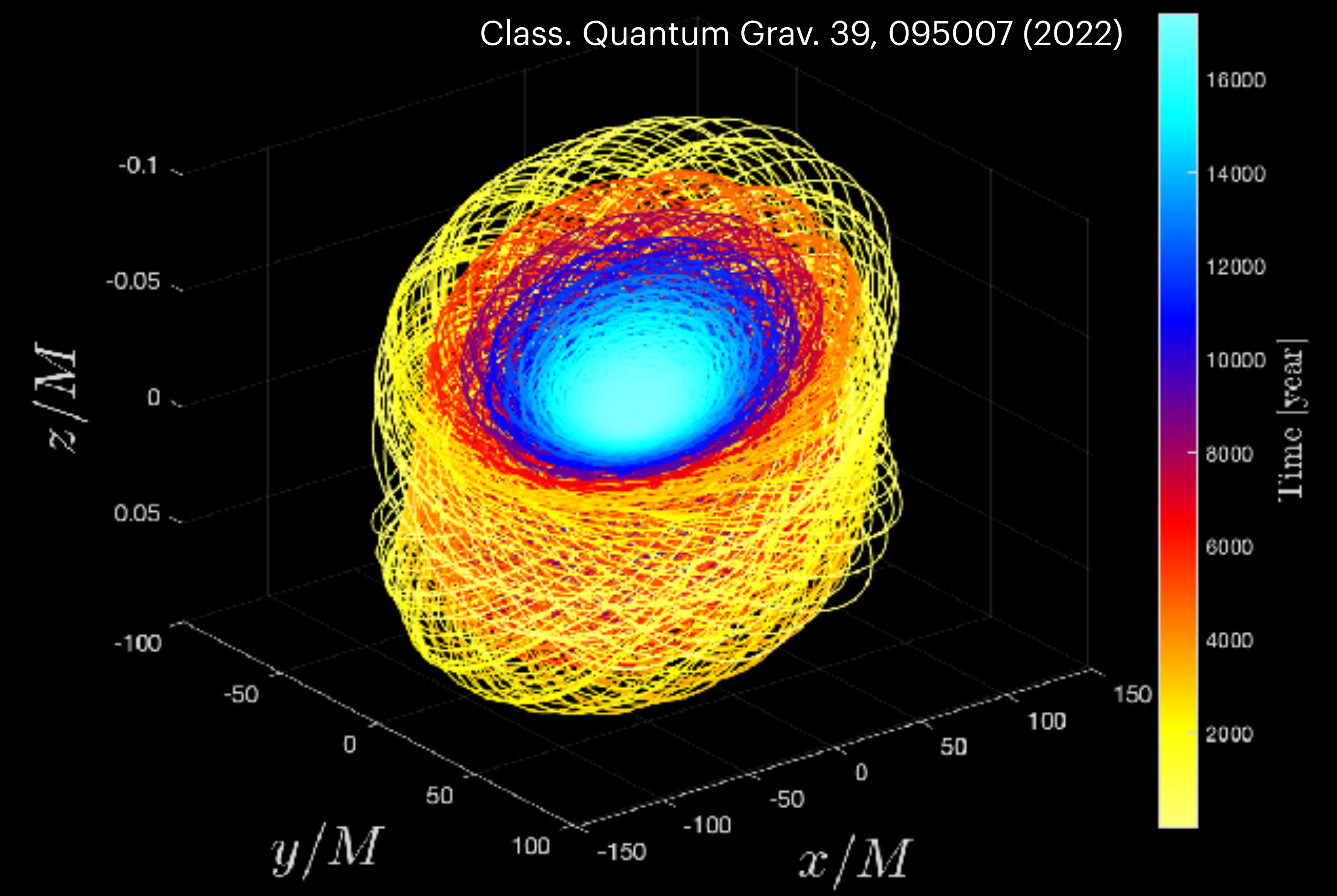

PRL 103, 131101 (2009)

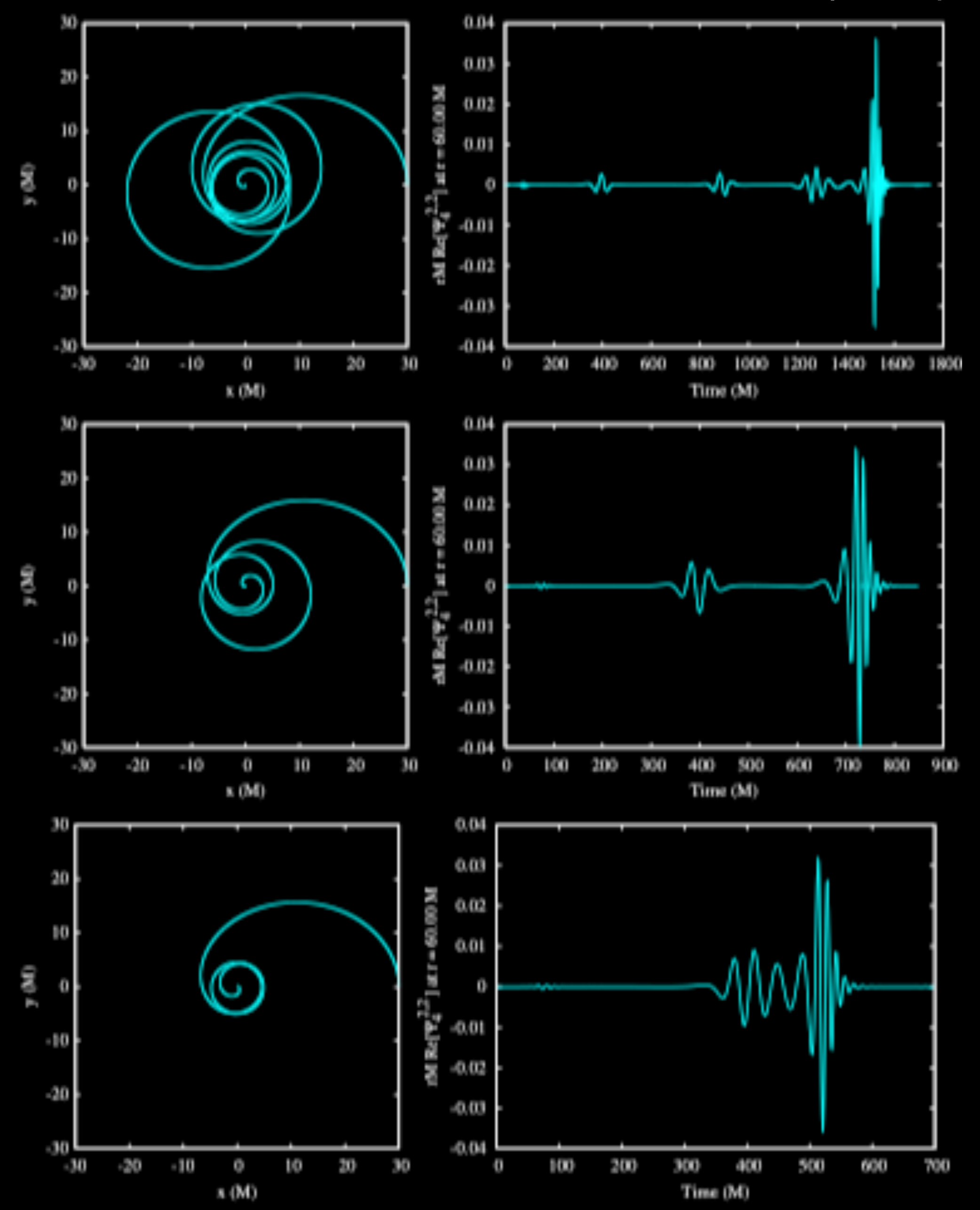

PRD 75, 124011 (2007)

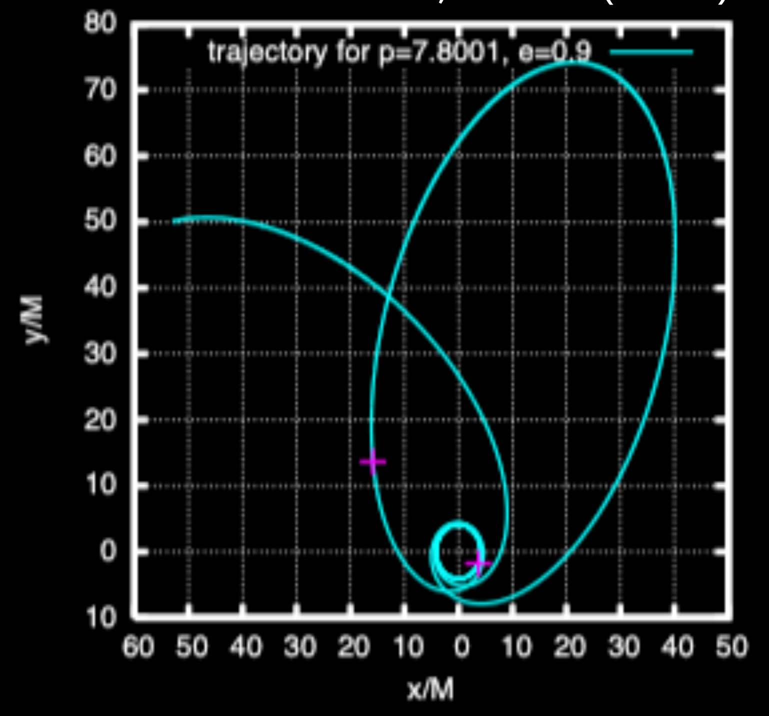

Algorithms Used in GW Search

- In the LAL library (used by the mainstream): Numerical, EOB, Taylor waveforms
- Excellently modeling the currently detectable waveforms
- Problems:
  - ➡Only short waveforms
  - ➡Only specific waveforms
  - ➡No eccentric waveforms
  - ➡Mostly spin-aligned

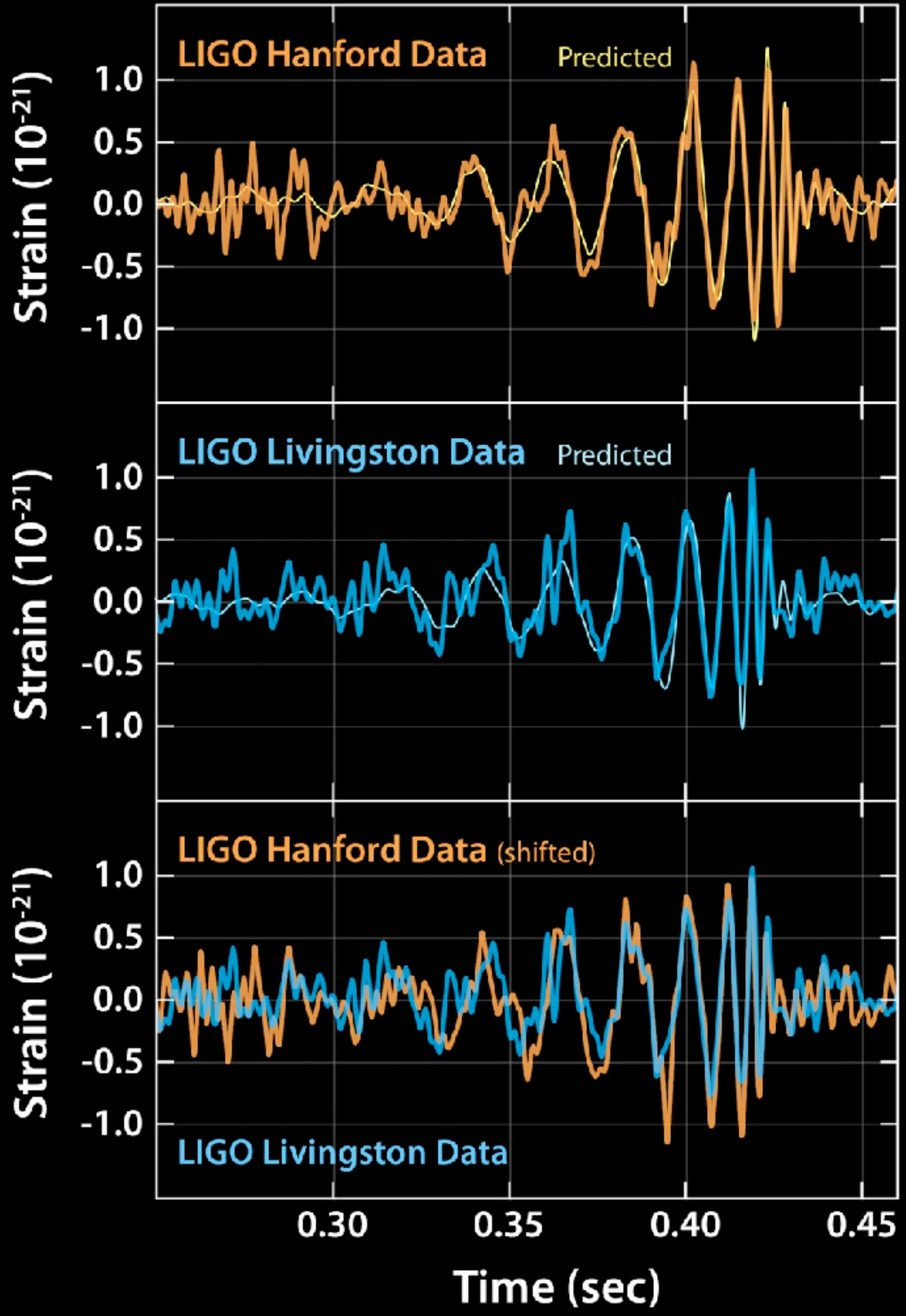

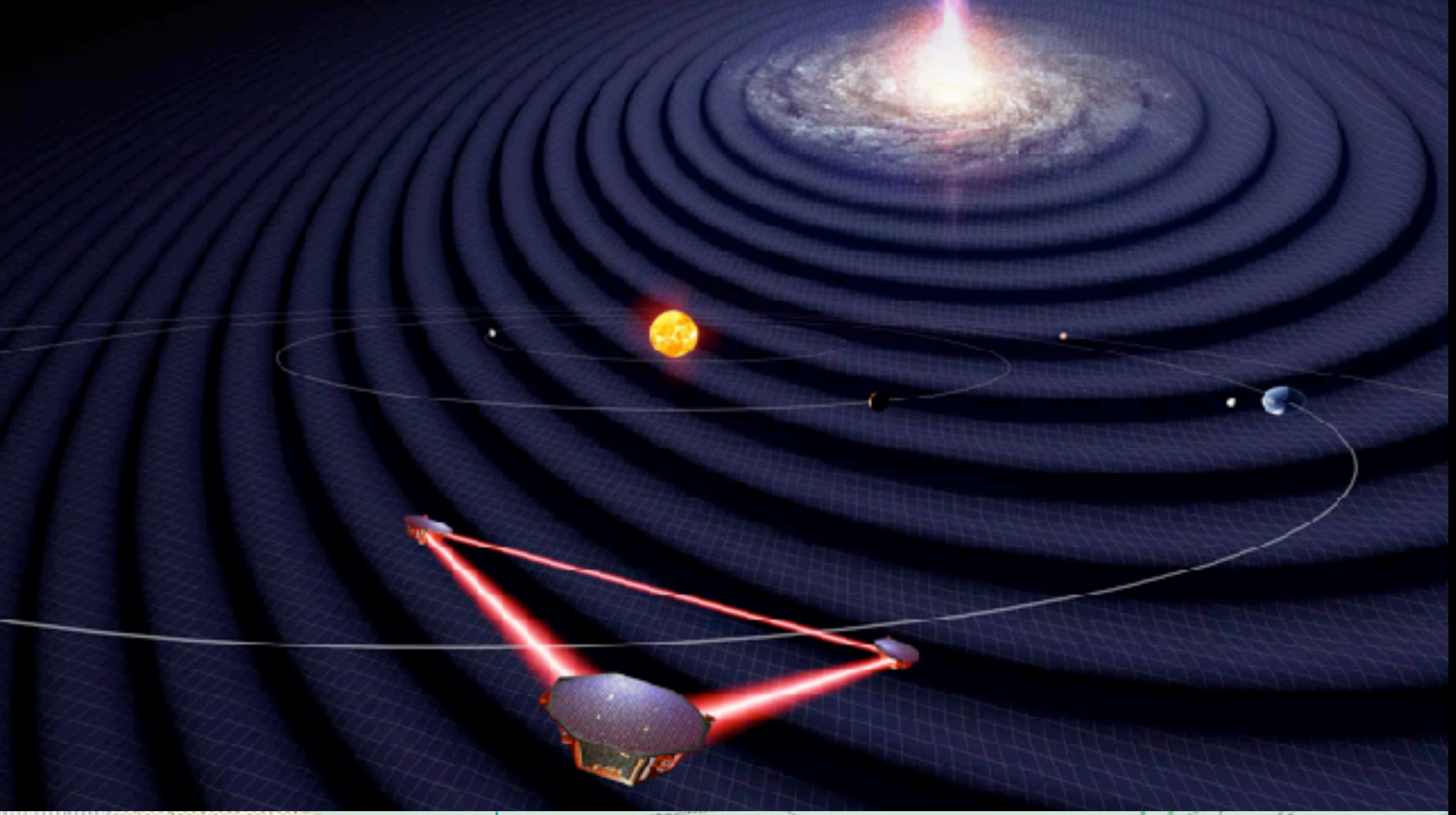

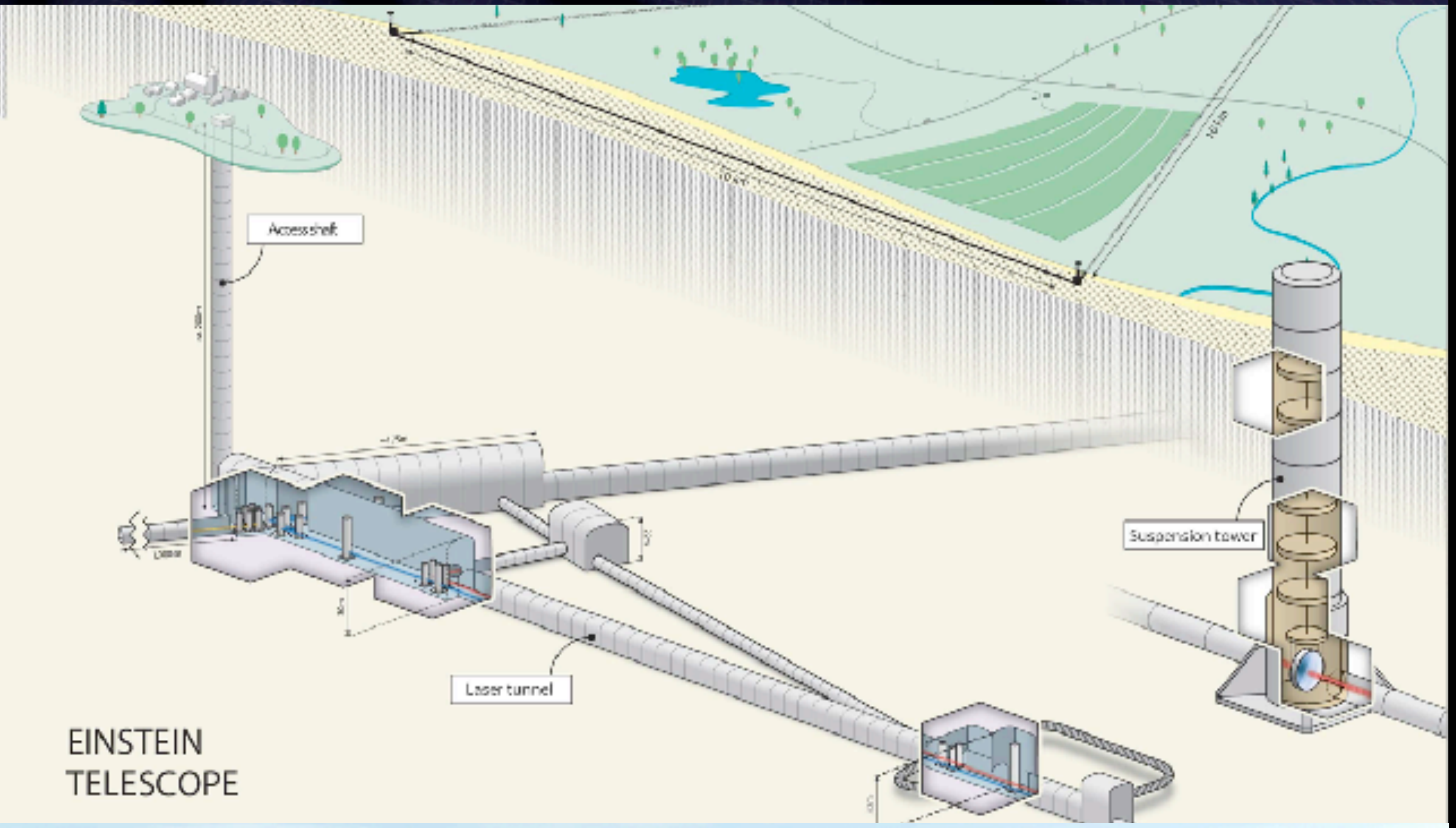

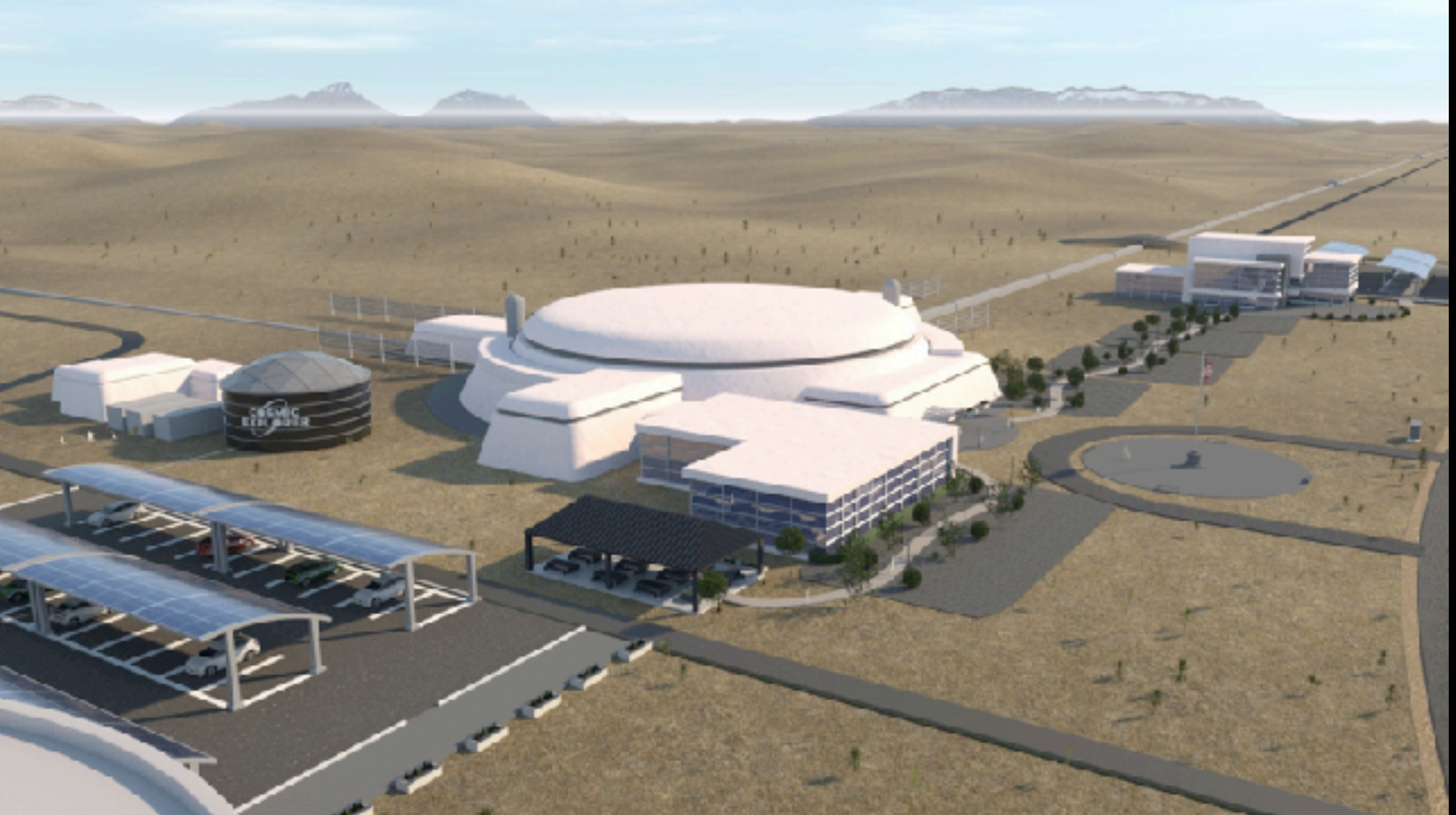

New GW Detectors on the Horizon

eLISA, Einstein Telescope, Cosmic Explorer

- Targeting new sources like NS-NS binaries, merging galactic nuclei, supernovae, stochastic background
- Significantly longer observational times ⟹ longer waveforms (up to 6 months — eLISA)
- Research of the inspiral phase
- Eccentricity and spin effects will be important in the orbital evolution of compact binaries
- eLISA got the green light this year

Gravitational Waves

Linearized theory

- Starting from the Einstein equation

$$R_{ab} - \frac{1}{2} g_{ab} R = \frac{8\pi G}{c^4} T^{ab}$$

- Take a small perturbation of the Einstein eq. around a flat spacetime (gauge symmetry of GR)

$$g_{ab} = \eta_{ab} + h_{ab}, \quad h_{ab} < < 1$$

- The Riemann-tensor expressed in h_{ab} linear order

$$R_{abcd} = \frac{1}{2}(\partial_b \partial_c h_{ad} + \partial_a \partial_d h_{bc} - \partial_a \partial_c h_{bd} - \partial_b \partial_d h_{ac})$$

- The linearized Einstein equation

$$\Box \bar{h}_{ab} + \eta_{ab} \partial^c \partial^d \bar{h}_{cd} - \partial^c \partial_b \bar{h}_{ac} - \partial^c \partial_a \bar{h}_{bc} = -\frac{16\pi G}{c^4} T_{ab}$$

- Using the gauge freedom of GR and choosing the De Donder gauge, $\partial^b \bar{h}_{ab} = 0$

$$\Box \bar{h}_{ab} = -\frac{16\pi G}{c^4} T_{ab}$$

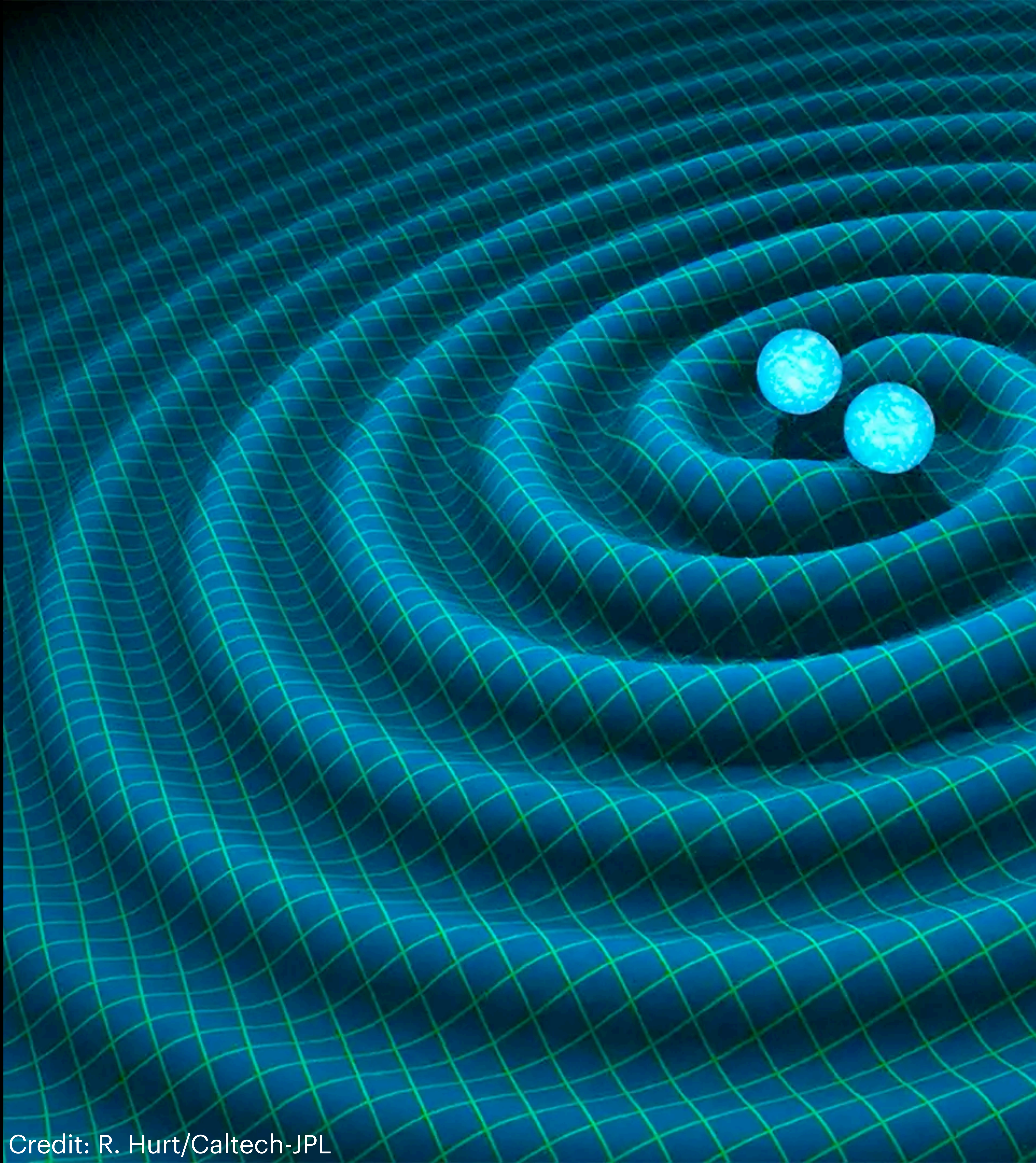

Credit: R. Hurt/Caltech-JPL

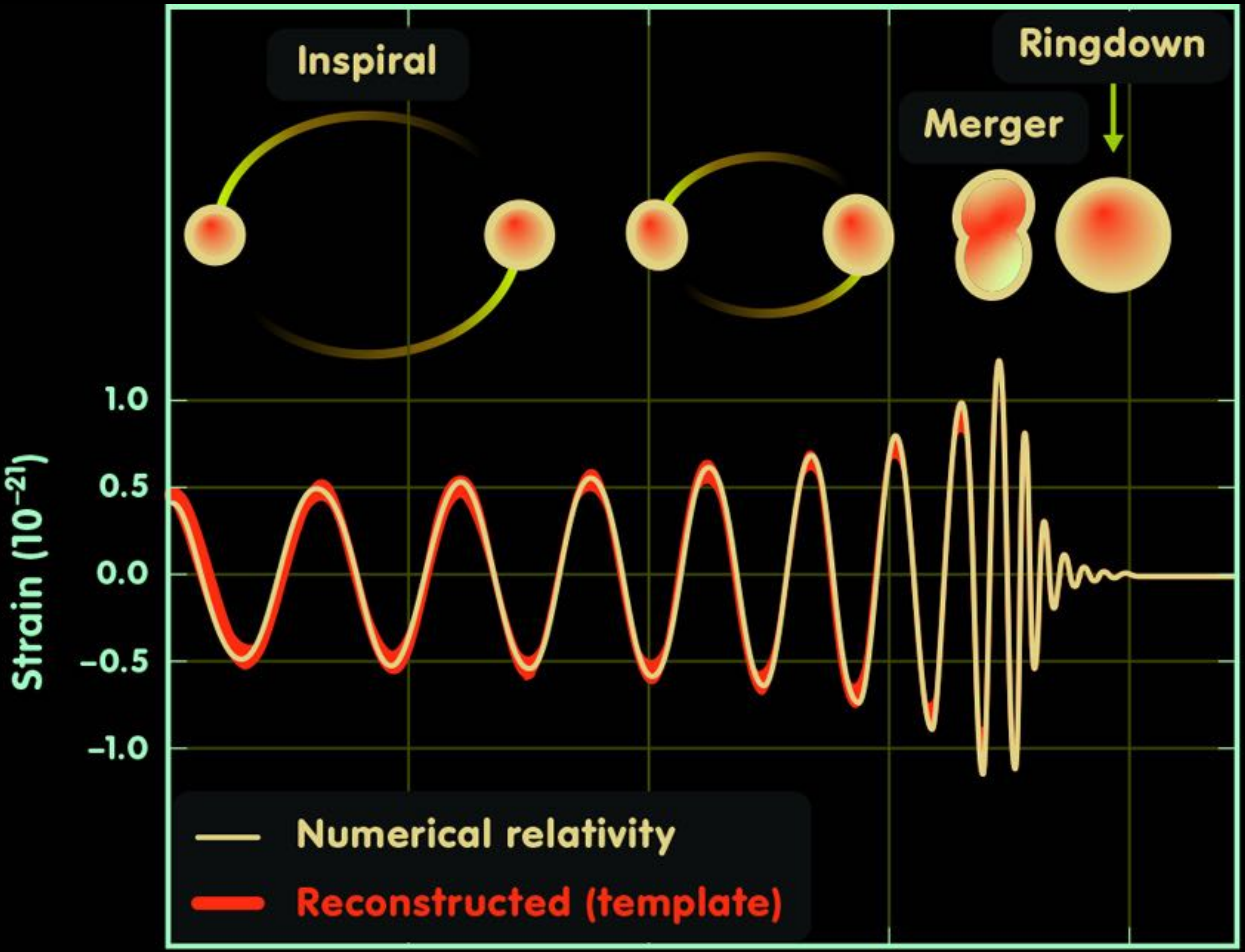

LIGO / Redesign: Daniela Leitner

Two-body problem of General Relativity

Maarten van de Meent - Own work

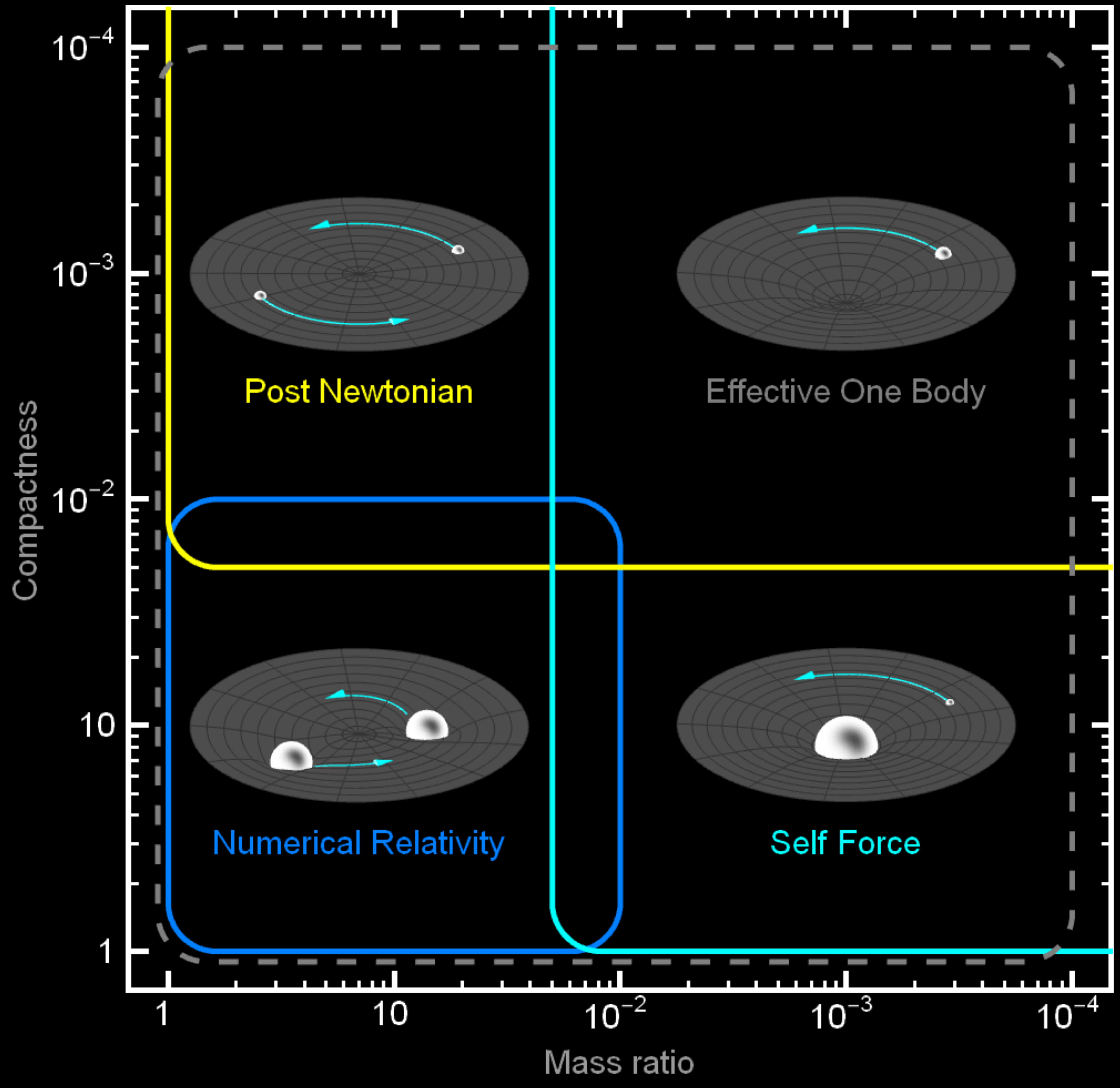

Post-Newtonian Expansion Used in CBWaves

- Built upon two assumptions:
  1. gravity inside the source is weak like in the post-Minkowsikian expansion
  2. the motion of the components of the source is slow
- The equation of motion

$$\mathbf{a} = \mathbf{a}_{\mathrm{N}} + \mathbf{a}_{\mathrm{PN}} + \mathbf{a}_{2\mathrm{PN}} + \mathbf{a}_{3\mathrm{PN}} + \mathbf{a}_{4\mathrm{PN}} + \underset{\mathrm{SO}}{\mathbf{a}}{}_{1.5\mathrm{PN}} + \underset{\mathrm{SS}}{\mathbf{a}}{}_{2\mathrm{PN}} + \underset{\mathrm{BT}}{\mathbf{a}}{}^{\mathrm{RR}}_{2.5\mathrm{PN}} + \underset{\mathrm{SO}}{\mathbf{a}}{}_{2.5\mathrm{PN}}$$

$$+ \underset{\mathrm{SO}}{\mathbf{a}}{}_{3.5\mathrm{PN}} + \underset{\mathrm{BT}}{\mathbf{a}}{}^{\mathrm{RR}}_{3.5\mathrm{PN}} + \underset{\mathrm{SS}}{\mathbf{a}}{}^{\mathrm{RR}}_{3.5\mathrm{PN}} + \underset{\mathrm{SO}}{\mathbf{a}}{}^{\mathrm{RR}}_{3.5\mathrm{PN}}$$

- The radiation field equation

$$h_{ij} = \frac{2G\mu}{c^4 D}[Q_{ij} + P^{0.5}Q_{ij} + PQ_{ij} + P^{1.5}Q_{ij} + P^2Q_{ij} + PQ_{ij}^{SO}$$

$$+P^{1.5}Q_{ij}^{SO} + P^2Q_{ij}^{SO} + PQ_{ij}^{SS} + P^{1.5}Q_{ij}^{tail}]$$

Effective One-Body Approach in SEOBNRE

- reduce the conservative dynamics of the general relativistic two-body problem
- Mathisson–Papapetrou–Dixon equation is taken on a deformed Kerr black hole
- Hamiltonian of the Mathisson–Papapetrou–Dixon equations:

$$H_{\text{eff}} = M\eta \left(\beta^i p_i + \alpha \sqrt{1 + \gamma^{ij} p_i p_j + Q_4(p)} + H_{\text{S}} \right) + H_{SC}$$

$$H = M \sqrt{1 + 2\eta \left(\frac{H_{\text{eff}}}{M\eta} - 1 \right)}$$

- In the EOBNR framework, the quasicircular part of the radiation field is divided into two:
  - the inspiral-plunge
  - post-merger phase

$$h_{lm}^{(C)} = h_{lm}^{(N,\epsilon)} \hat{S}_{\text{eff}}^{(\epsilon)} T_{lm} e^{i\delta_{lm}} (\rho_{lm})^l N_{lm}$$

$$h_{lm}^{(N,\epsilon)} = \frac{M\eta}{D} n_{lm}^{(\epsilon)} c_{l+\epsilon} V_\Phi^l Y^{l-\epsilon,-m} \left(\frac{\pi}{2}, \Phi \right)$$

- For the eccentric part, in the radiation field terms up to the second post-Newtonian order are considered

Numerical Results

- 2 codes were used; one based on the PN, `CBwaves`; and one based on EOB, `SEOBNRE`
- both codes use a 4th-order Runge—Kutta integrator
- on an identical initial parameter space

Initial Parameters

m_1 [$M_\odot$]	10 … 100
m_2 [$M_\odot$]	10 … 100
R [M_{tot}]	30
R_{min} [M_{tot}]	6
e_0	0.003
dt [sec]	1/4096

- `SEOBNRE` uses the initial orbital frequency: $f_{\text{init}} = \dfrac{c^3}{\pi G(m_1 + m_2)M_\odot\sqrt{\mathbf{r}_0^3}}$

Evolution of the orbital separation with 5 Hz initial orbital frequency at q = 1/100

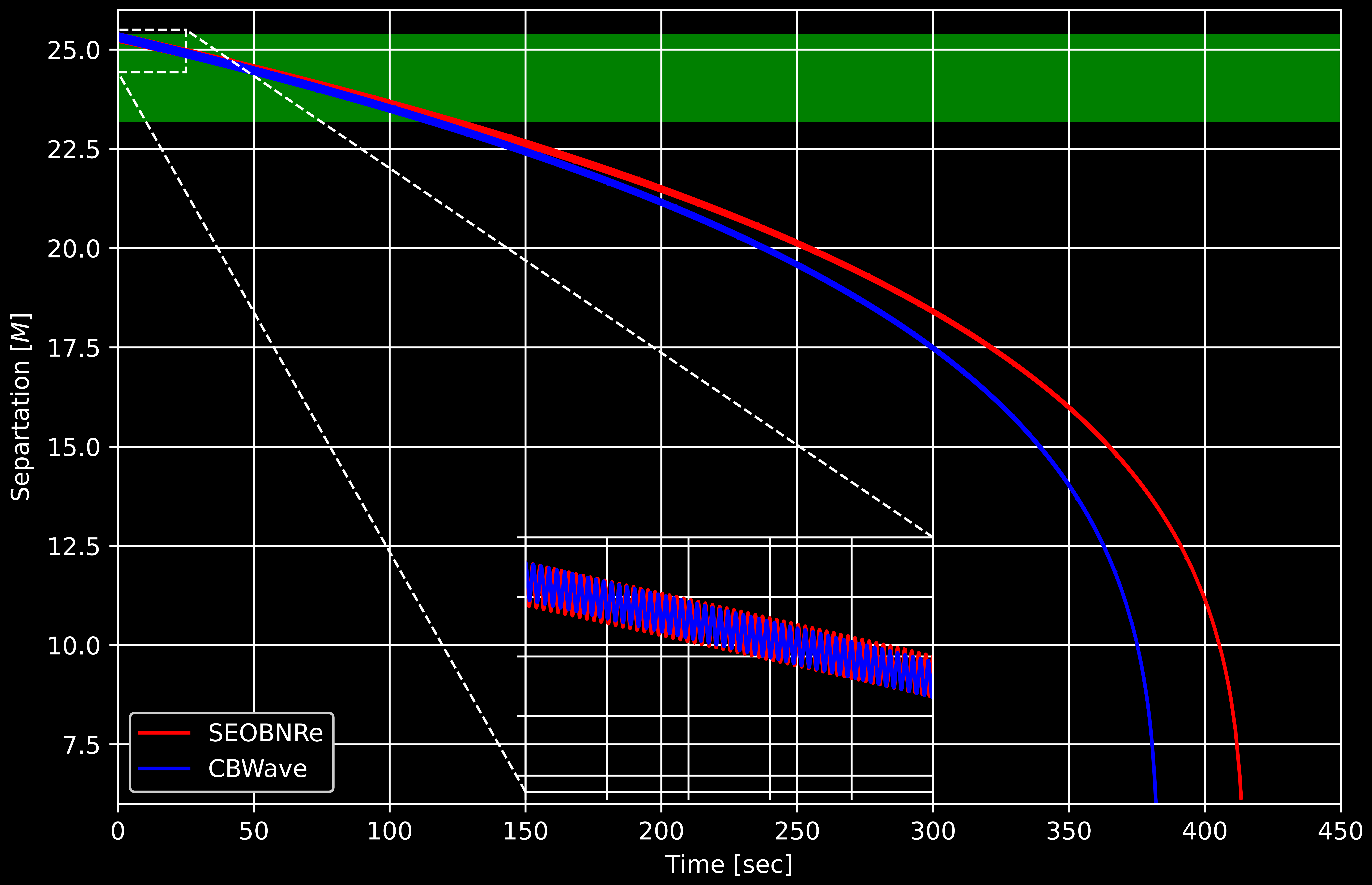

Evolution of the orbital separation with 5 Hz initial orbital frequency

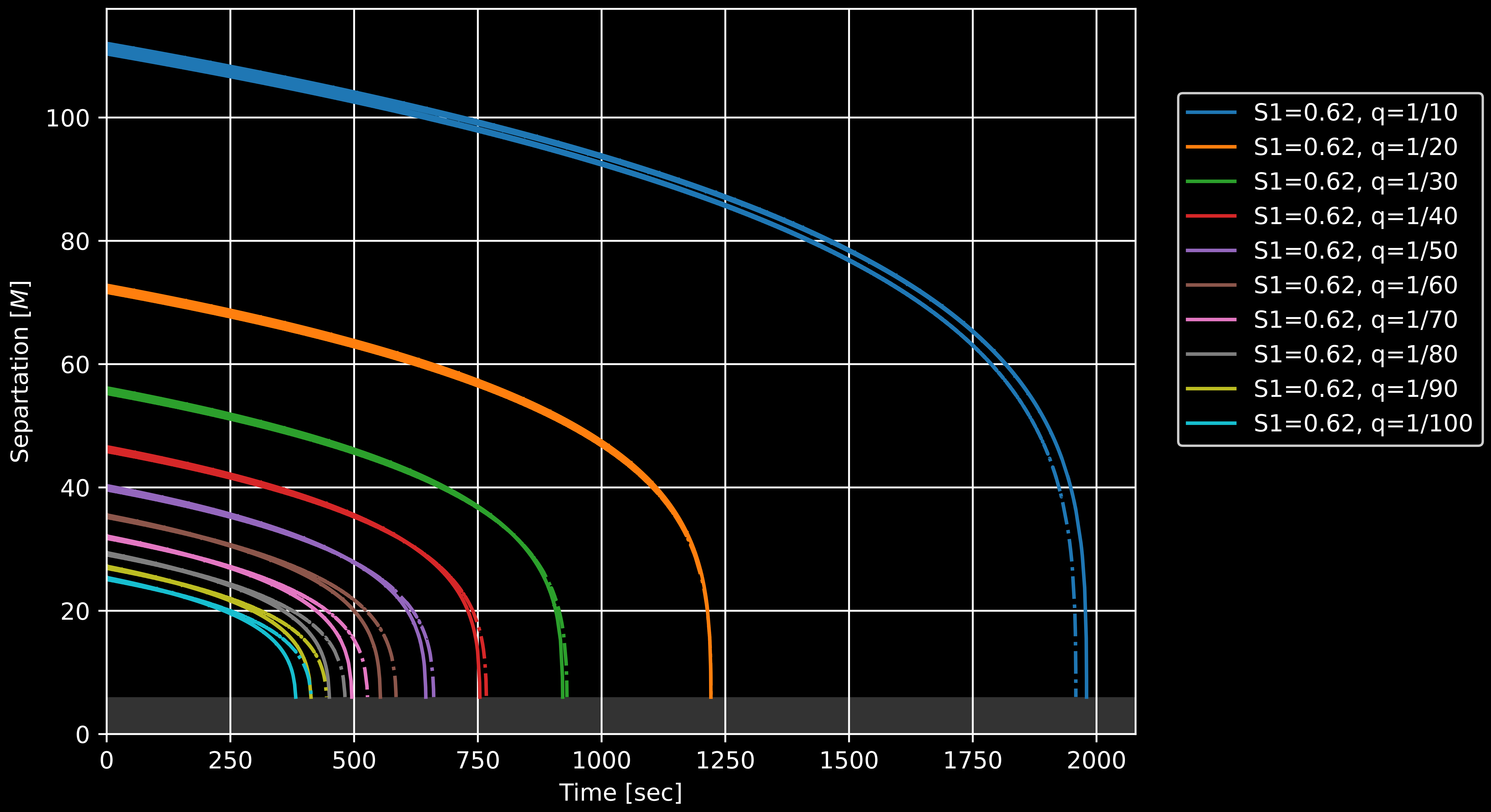

Mismatch/Unfaithfulness

- To calculate the mismatch, one first has to calculate the Overlap:

$$\mathcal{O} = \frac{\left\langle h_1, h_2 \right\rangle}{\sqrt{\left\langle h_1, h_1 \right\rangle \left\langle h_2, h_2 \right\rangle}}$$

where

$$\left\langle h_1, h_2 \right\rangle = 4\Re \int_{f_{\max}}^{f_{\min}} \frac{\tilde{h}_1 \tilde{h}_2^{\,*}}{S_n(f)} \mathrm{d}f$$

- The mismatch (or unfaithfulness) is the marginalized overlap over some quantities

$$\mathcal{M} = 1 - \max_{t,\phi,\psi} \mathcal{O}(h_1, h_2)$$

where the $\max$ was taken over timeshifts, polarization angles, and phase

- The `kuibit` was used.

Mismatch map for the not-spinning configurations

m₁ = 44.5455 M☉, m₂ = 39.0909 M☉ and q = 0.8775499209

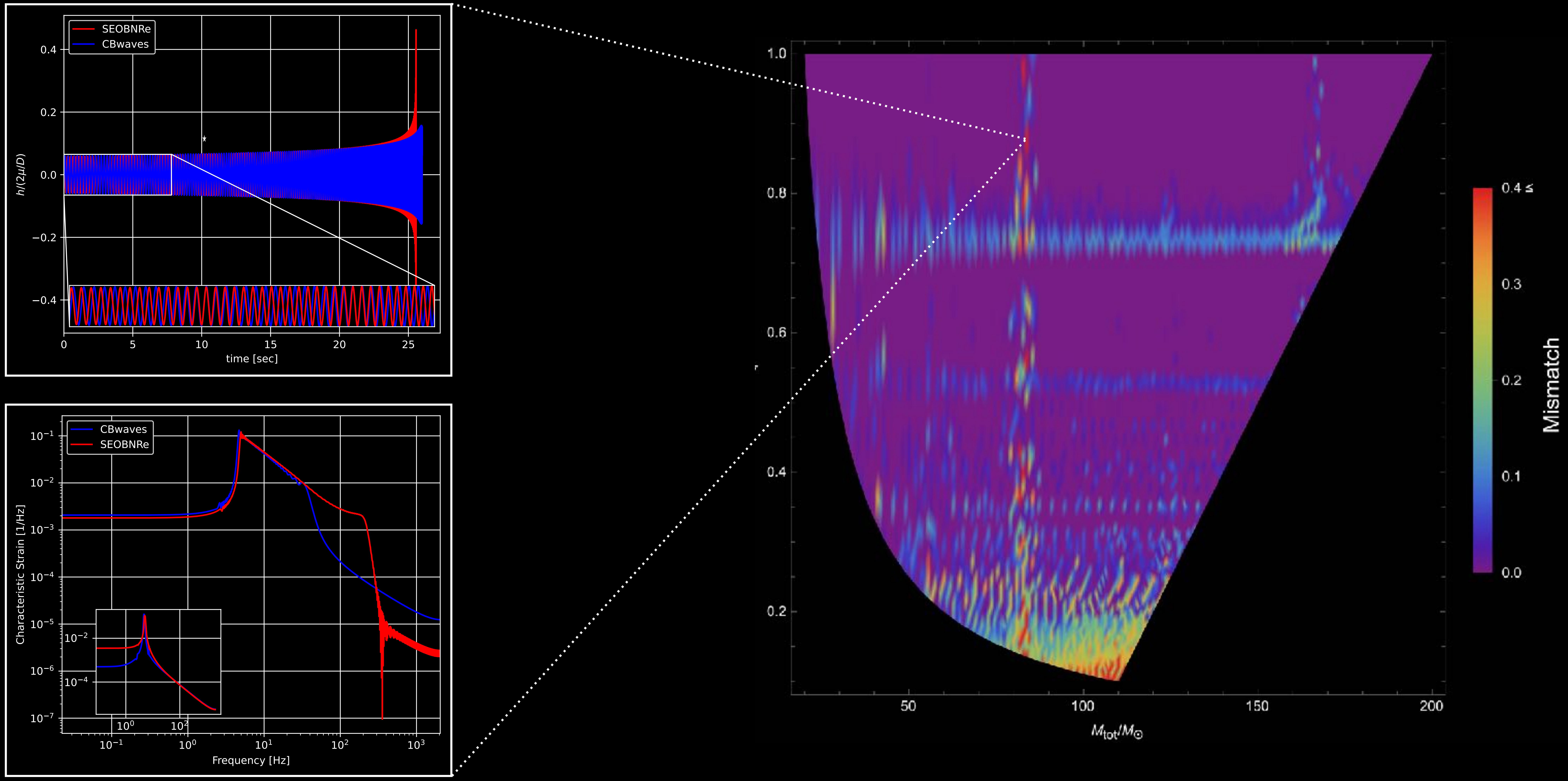

Mismatch map for the spin-aligned configurations

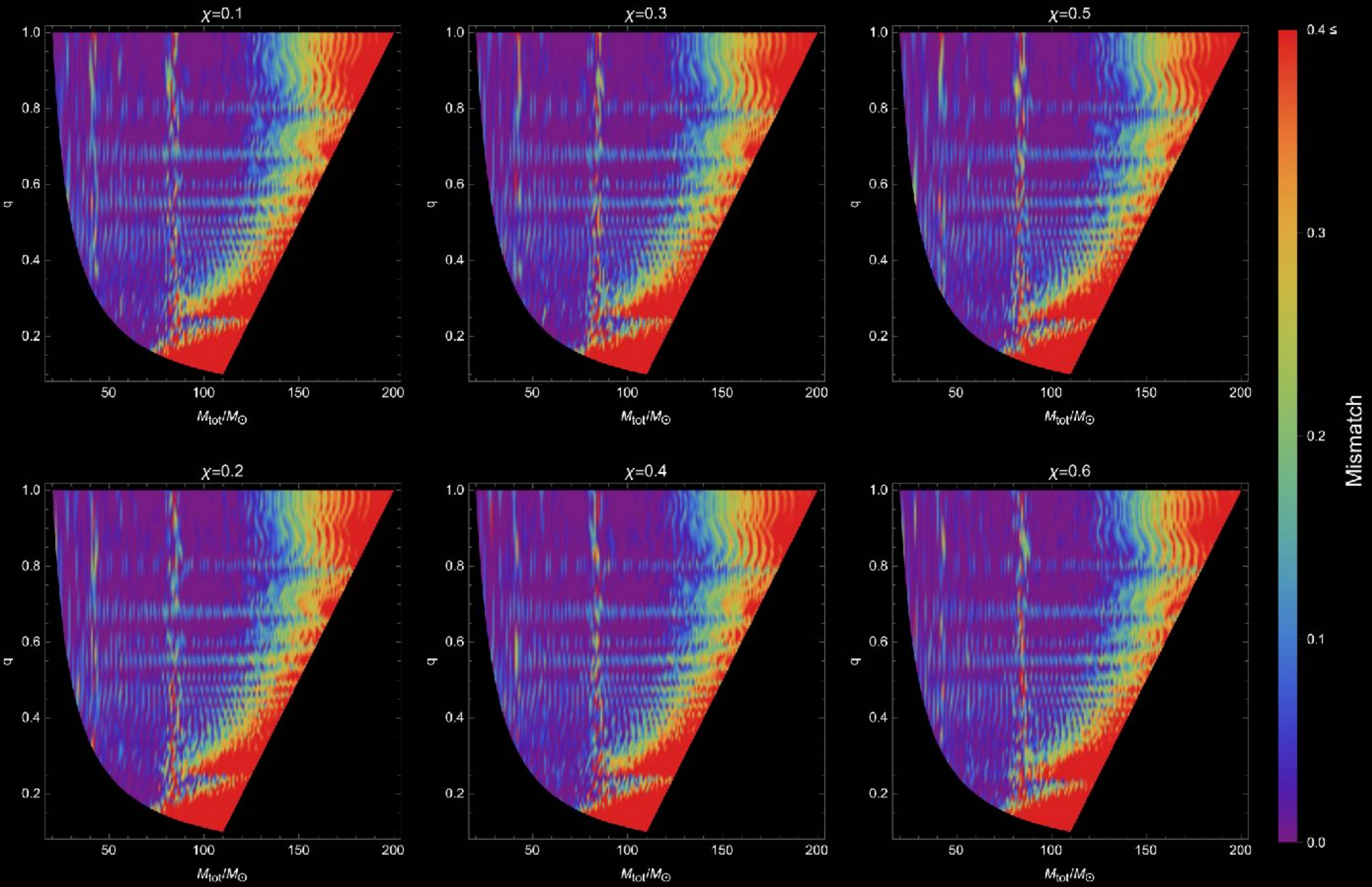

Mismatch map for the non-aligned spin configurations

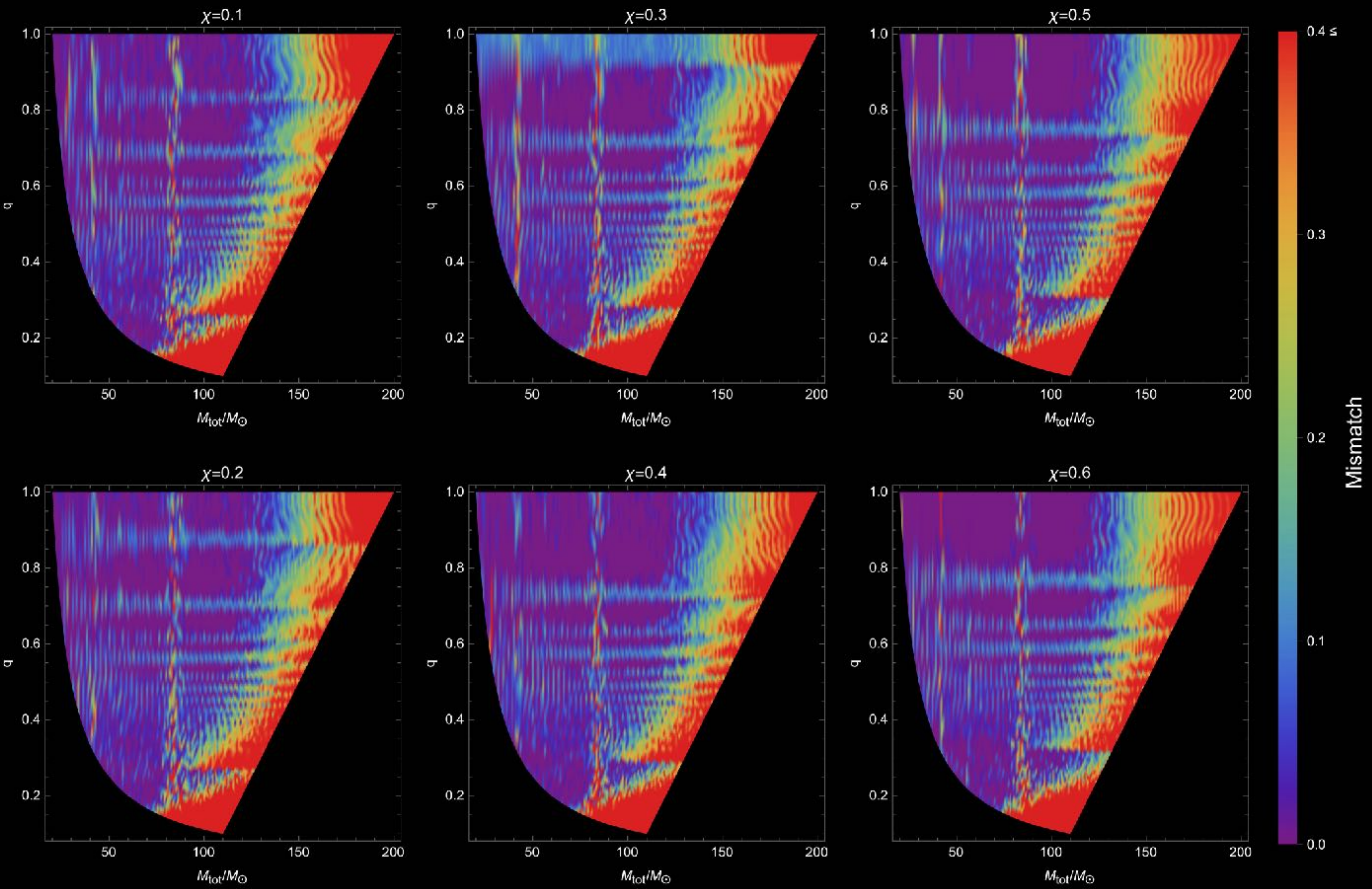

Orbital evolution of the binary at $\chi_1 = 0.6$, $m_1 = m_2 = 10\ \mathrm{M}_\odot$

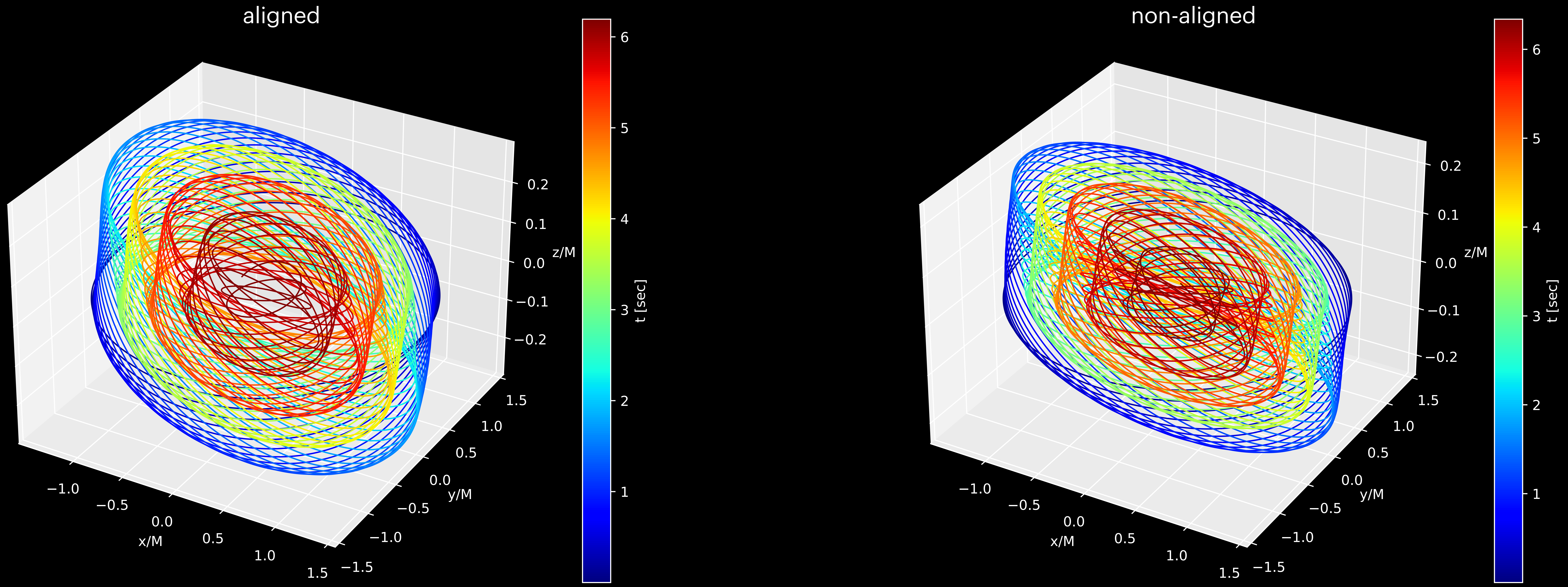

not-spinning, $m_2 = 10\ M_\odot$, $m_2 = 10\ M_\odot$

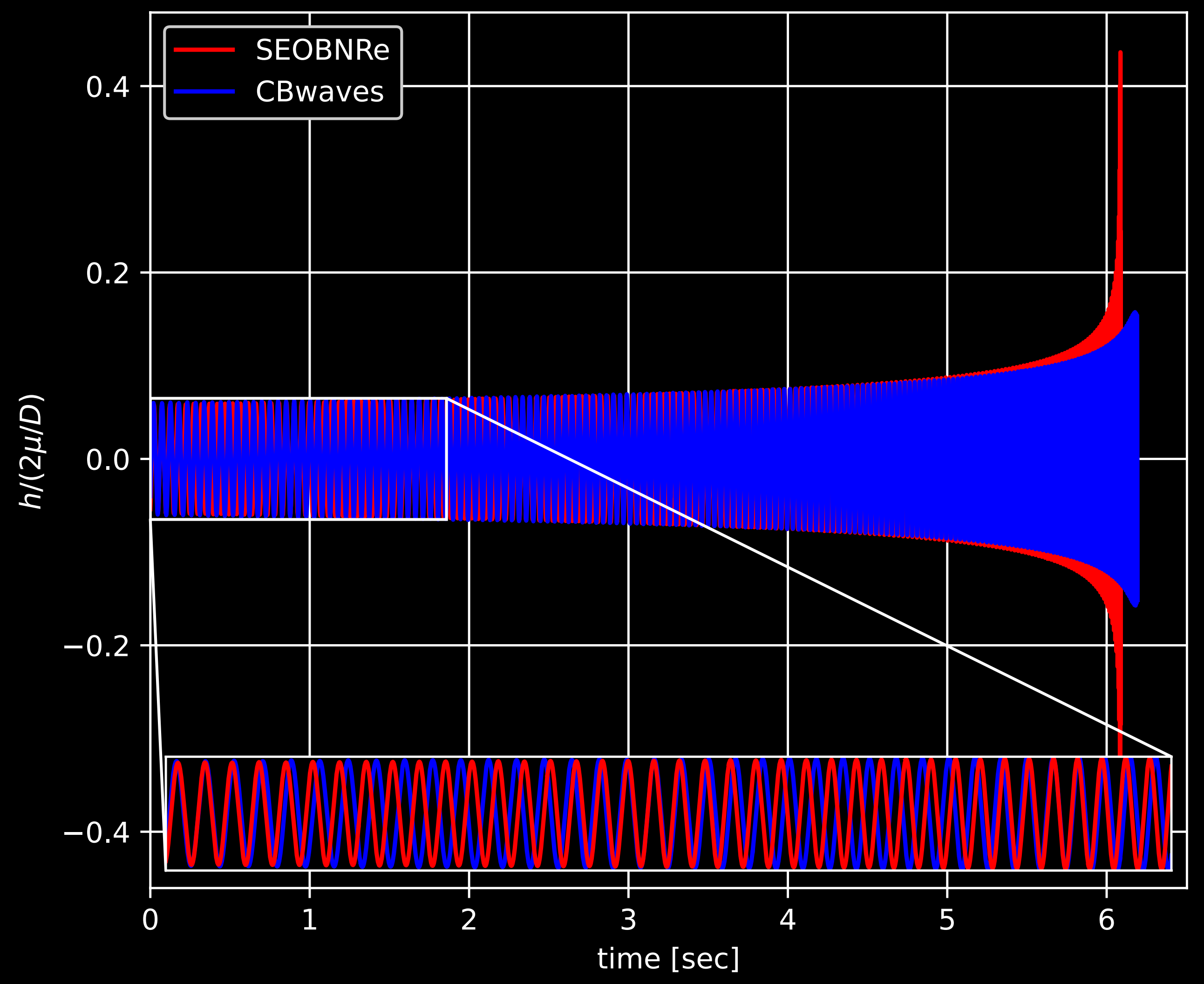

not-spinning, $m_2 = 100\ M_\odot$, $m_2 = 10\ M_\odot$

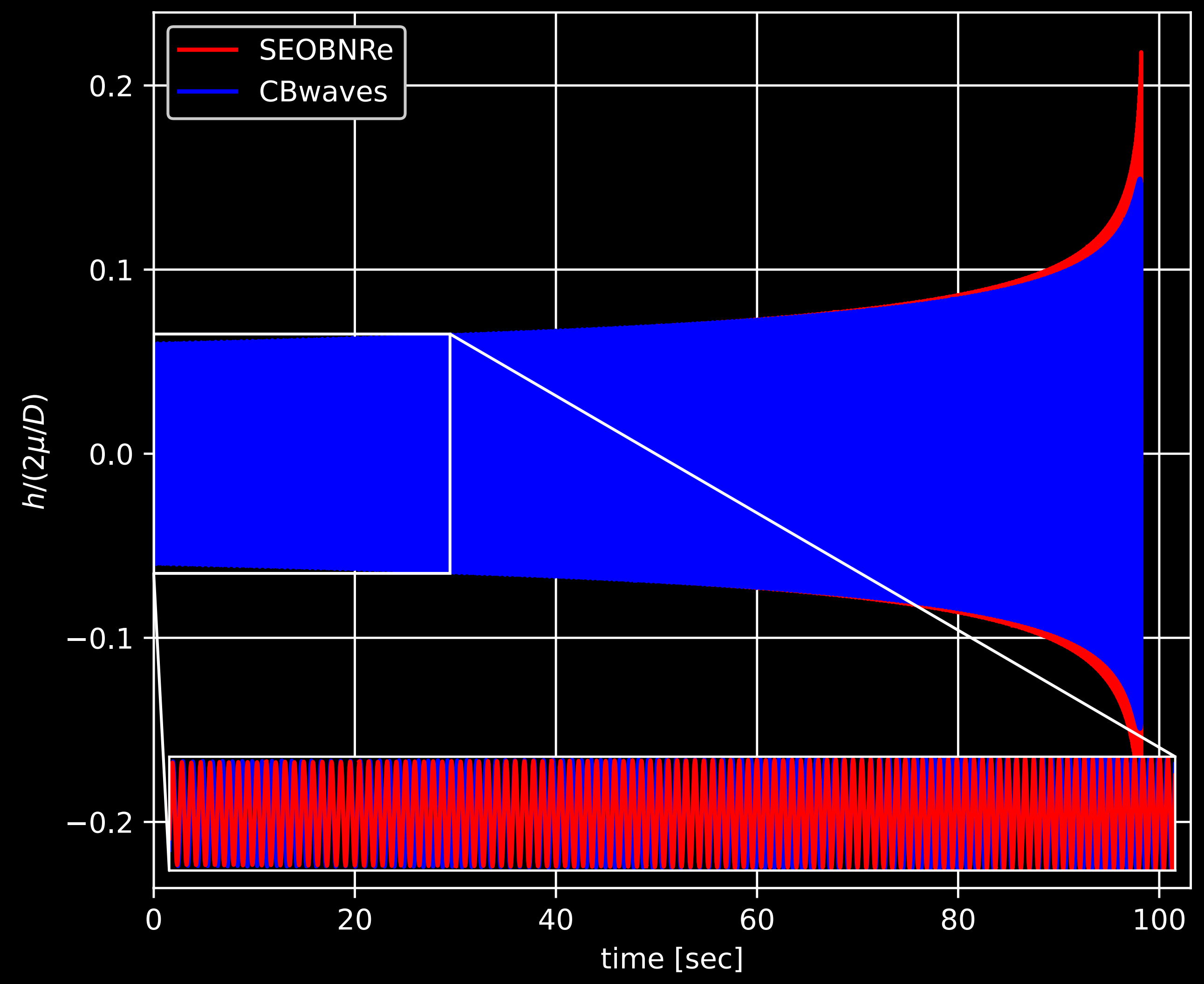

$\chi_1 = 0.6$, aligned, $m_2 = 10\ M_\odot$, $m_2 = 10\ M_\odot$

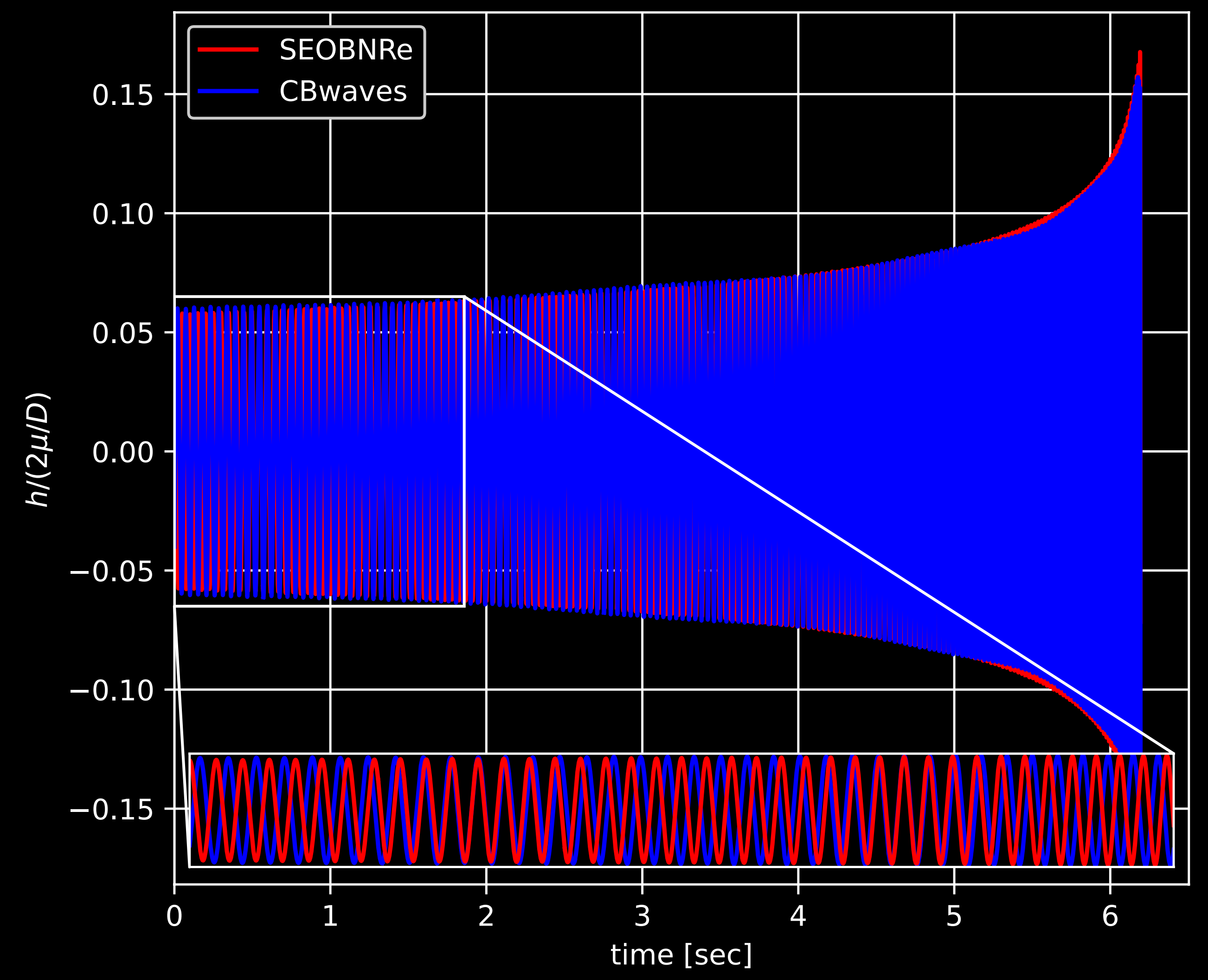

$\chi_1 = 0.6$, aligned, $m_2 = 100\ M_\odot$, $m_2 = 10\ M_\odot$

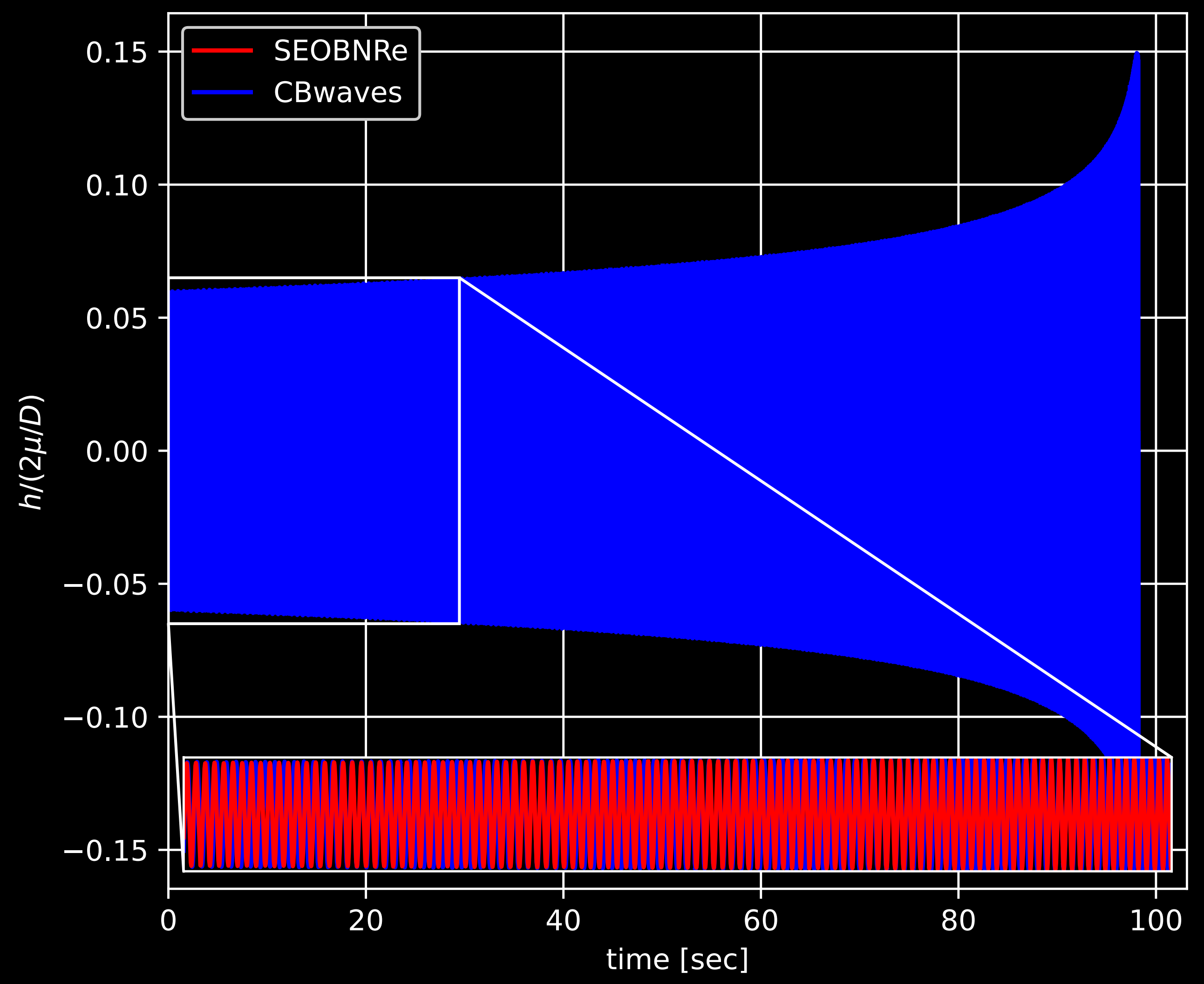

$\chi_1 = 0.6$, ~~aligned~~, $m_2 = 10\ M_\odot$, $m_2 = 10\ M_\odot$

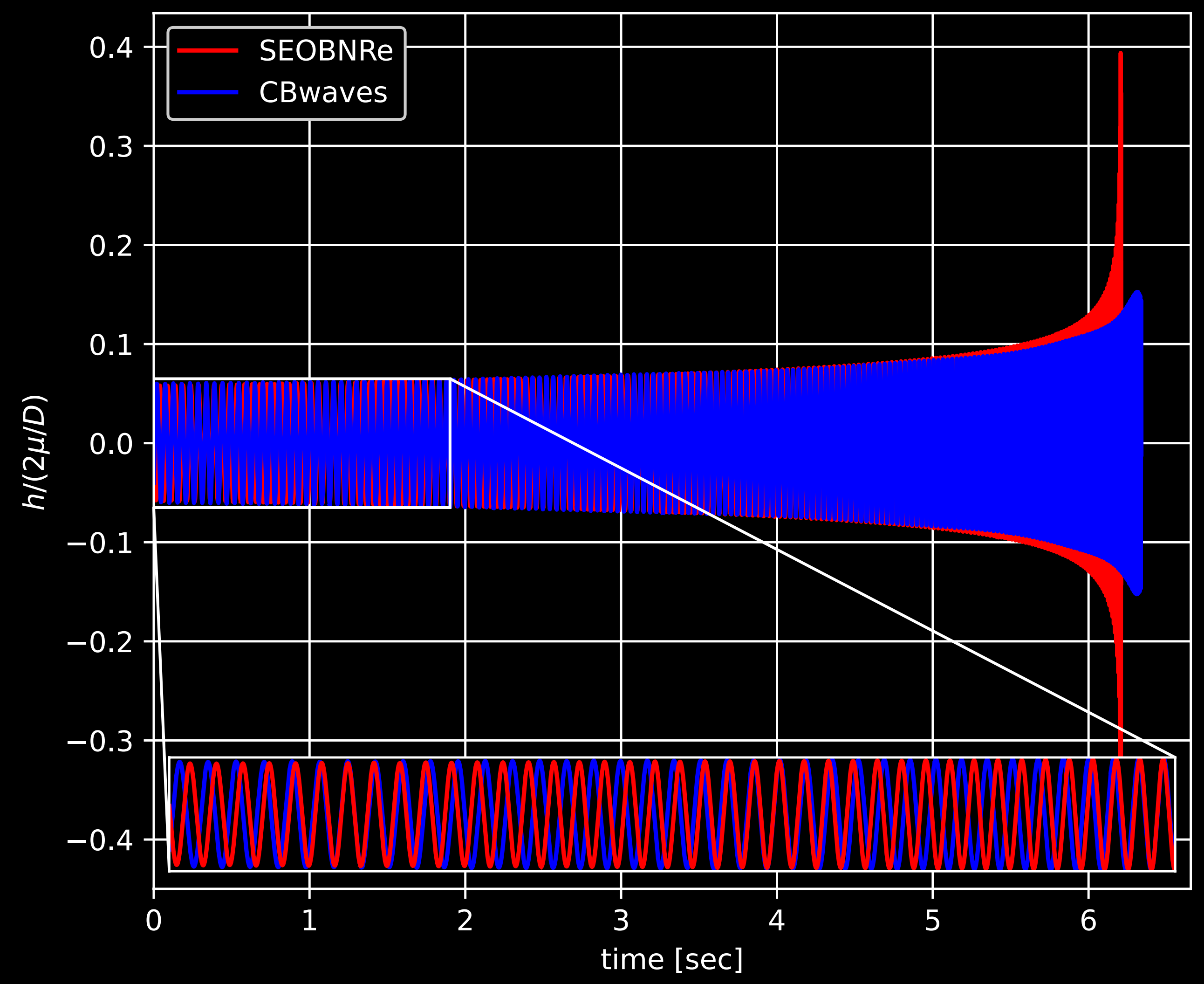

$\chi_1 = 0.6$, ~~aligned~~, $m_2 = 100\ M_\odot$, $m_2 = 10\ M_\odot$

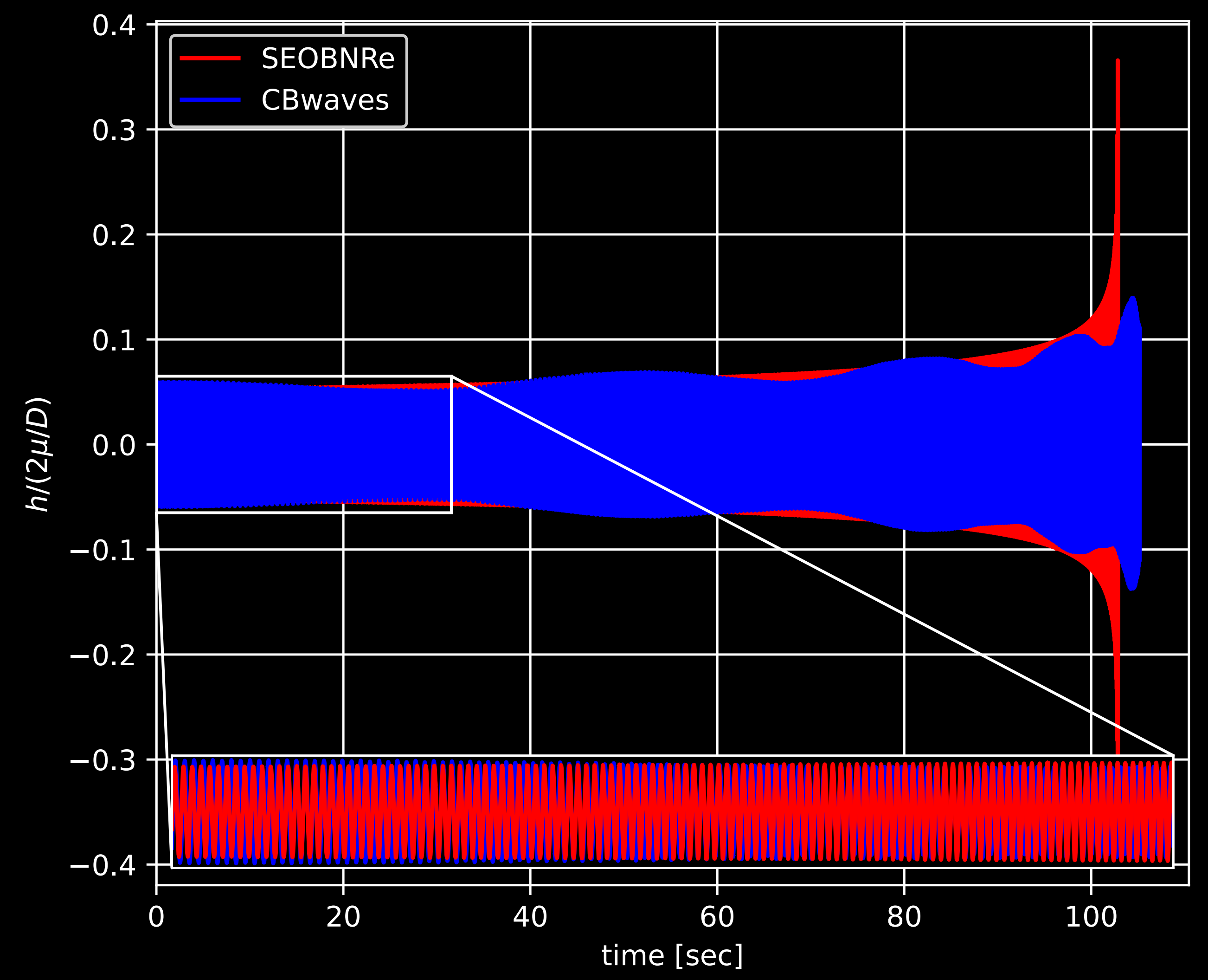

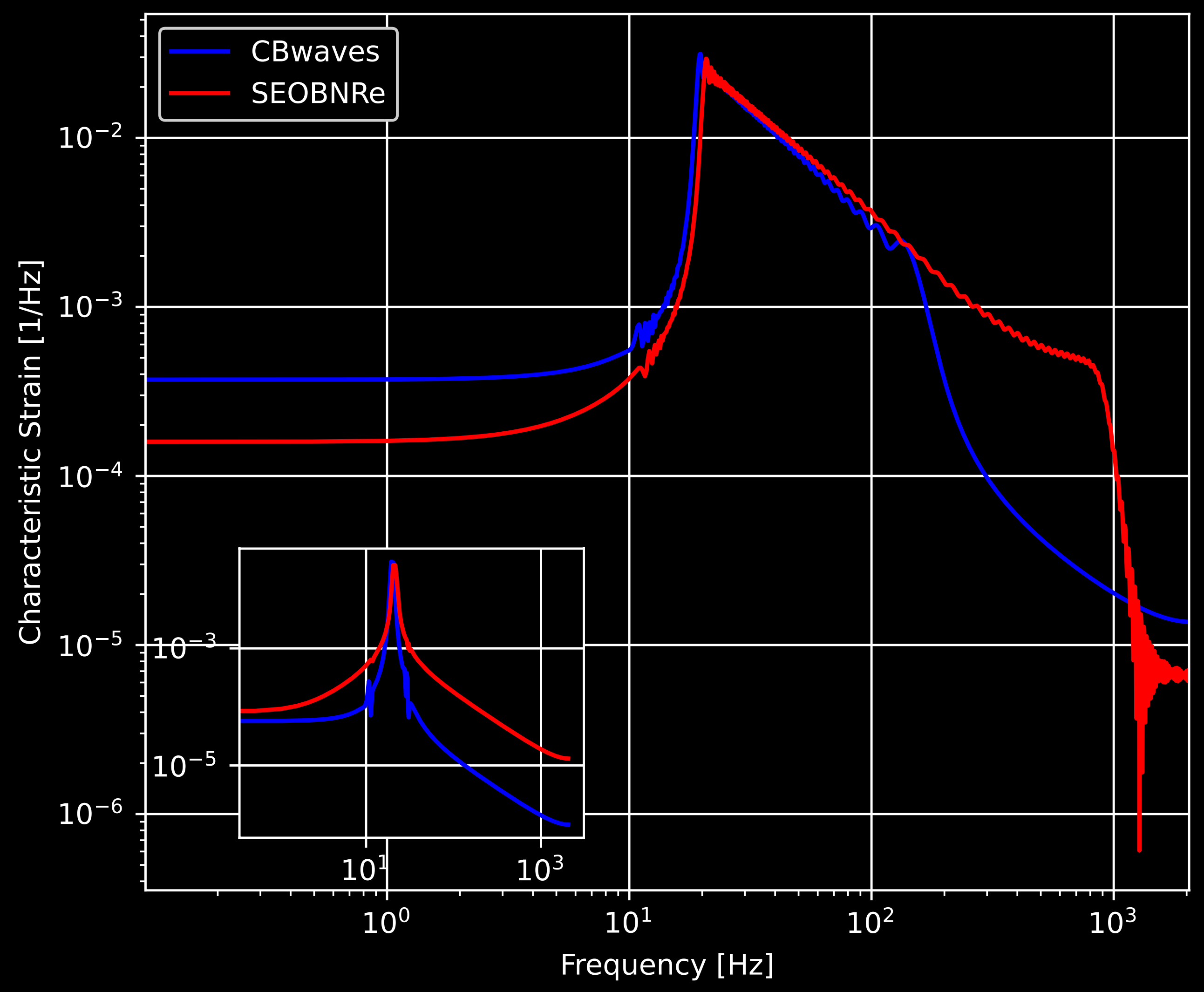

not-spinning, $m_2 = 10\ M_\odot$, $m_2 = 10\ M_\odot$

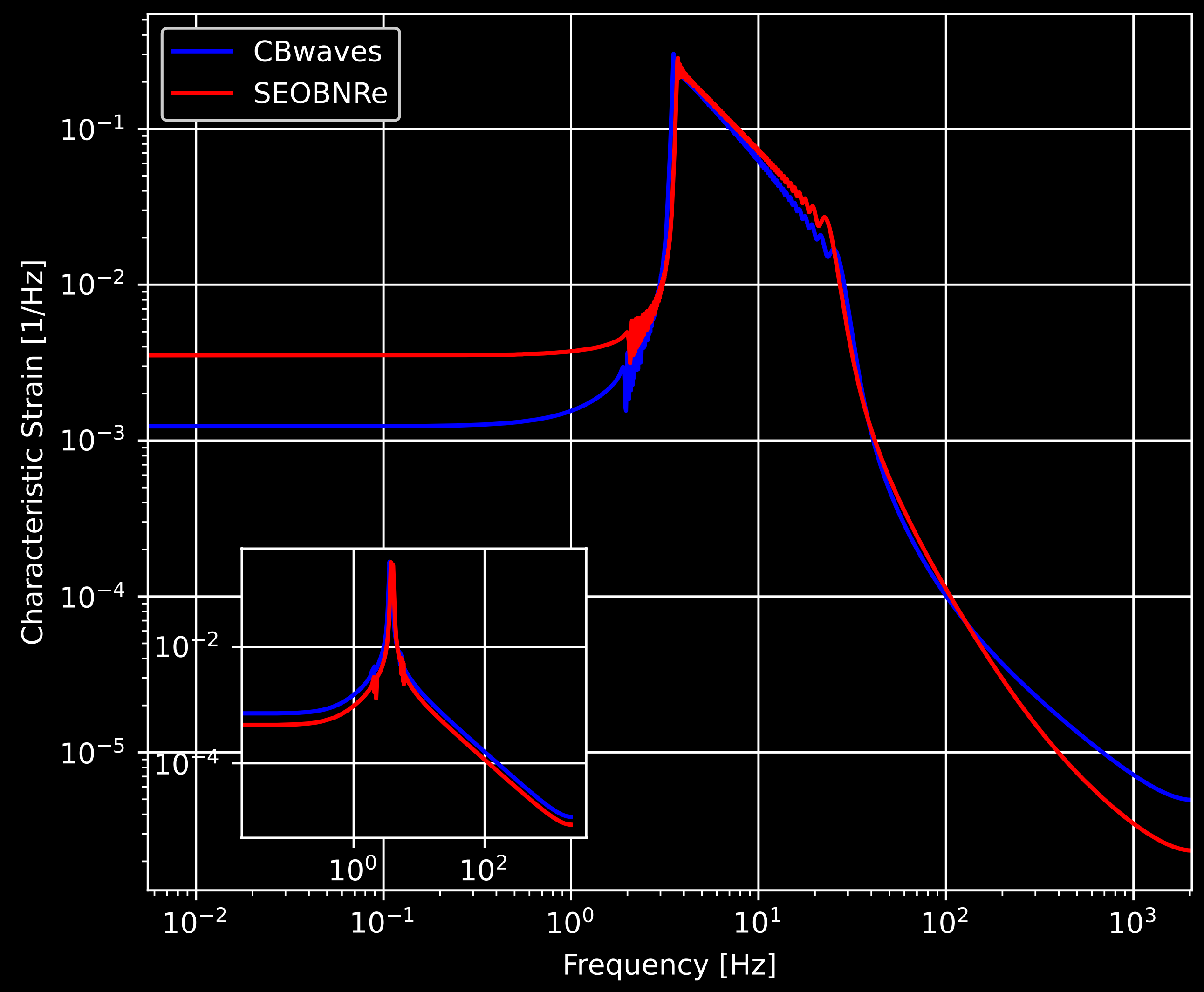

not-spinning, $m_2 = 100\ M_\odot$, $m_2 = 10\ M_\odot$

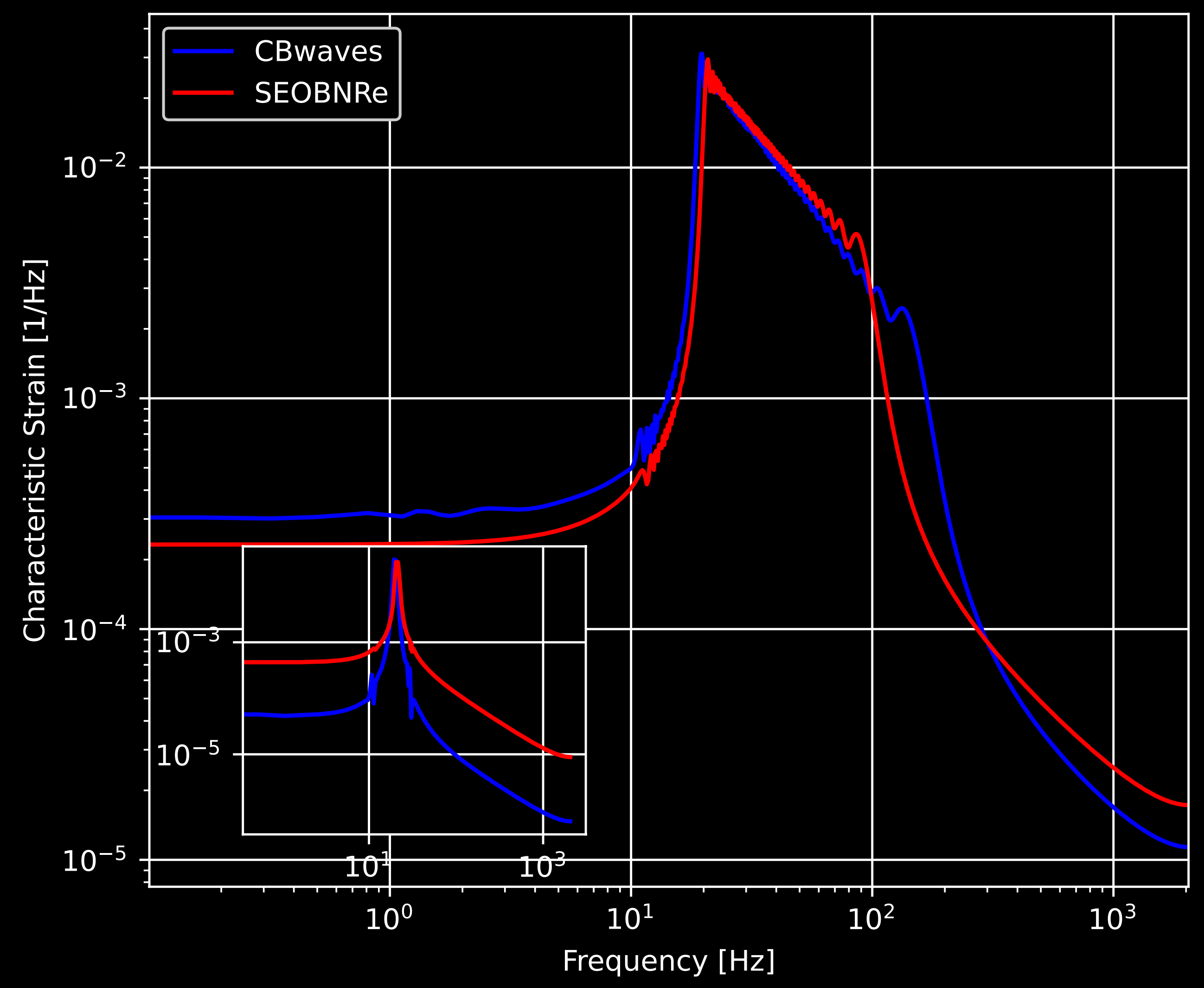

$\chi_1 = 0.6$, aligned, $m_2 = 10\ M_\odot$, $m_2 = 10\ M_\odot$

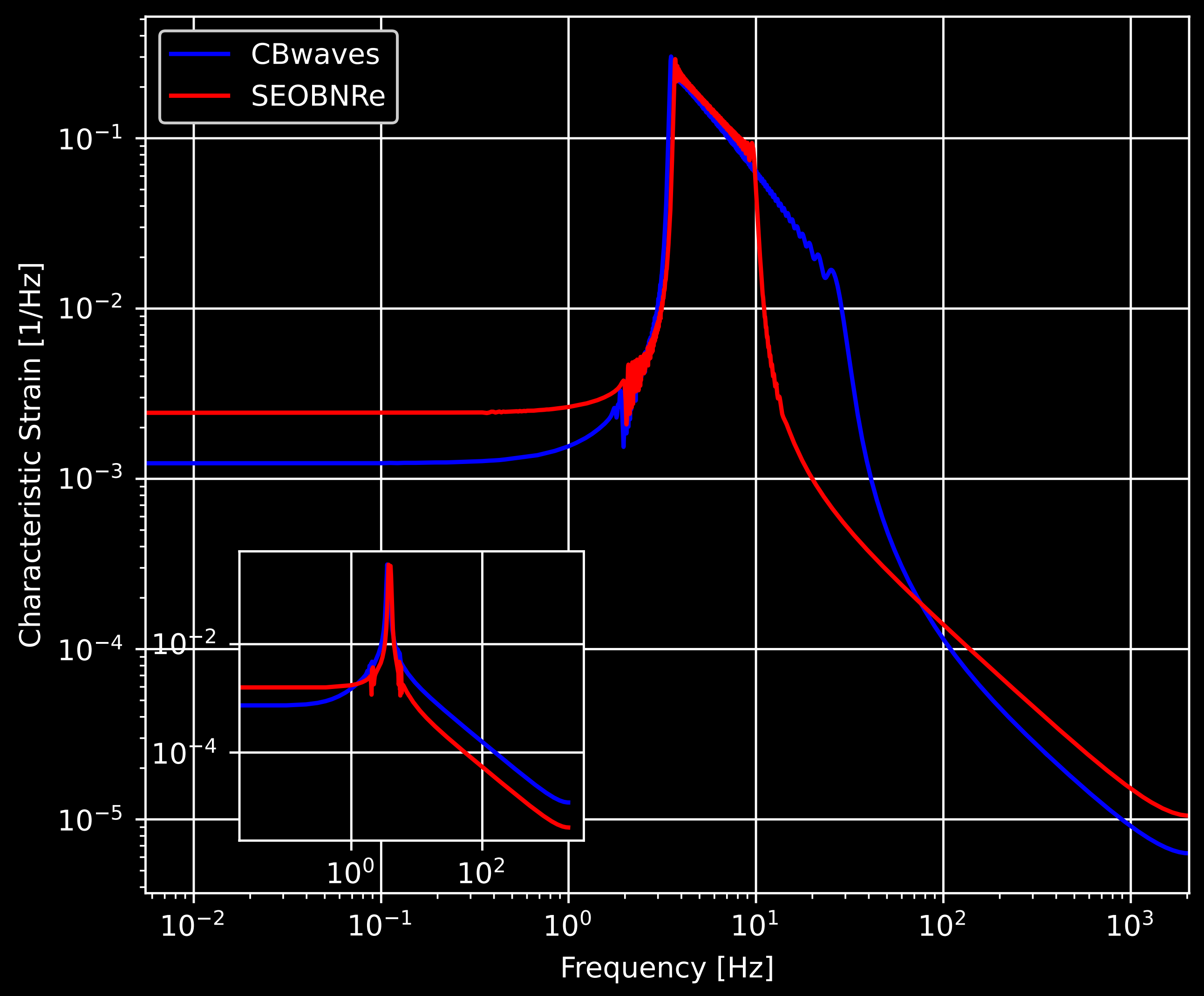

$\chi_1 = 0.6$, aligned, $m_2 = 100\ M_\odot$, $m_2 = 10\ M_\odot$

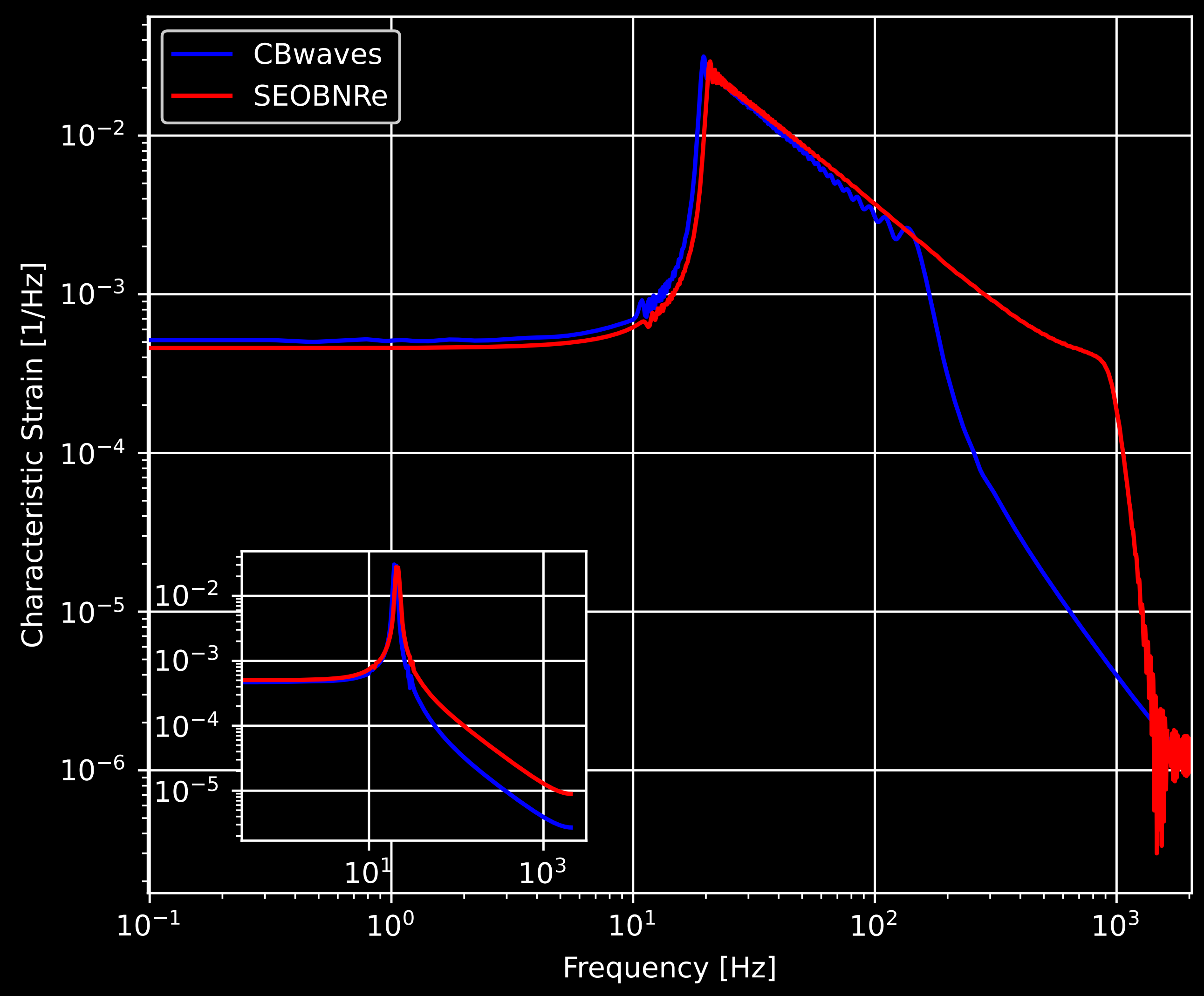

$\chi_1 = 0.6$, ~~aligned~~, $m_2 = 10\ M_\odot$, $m_2 = 10\ M_\odot$

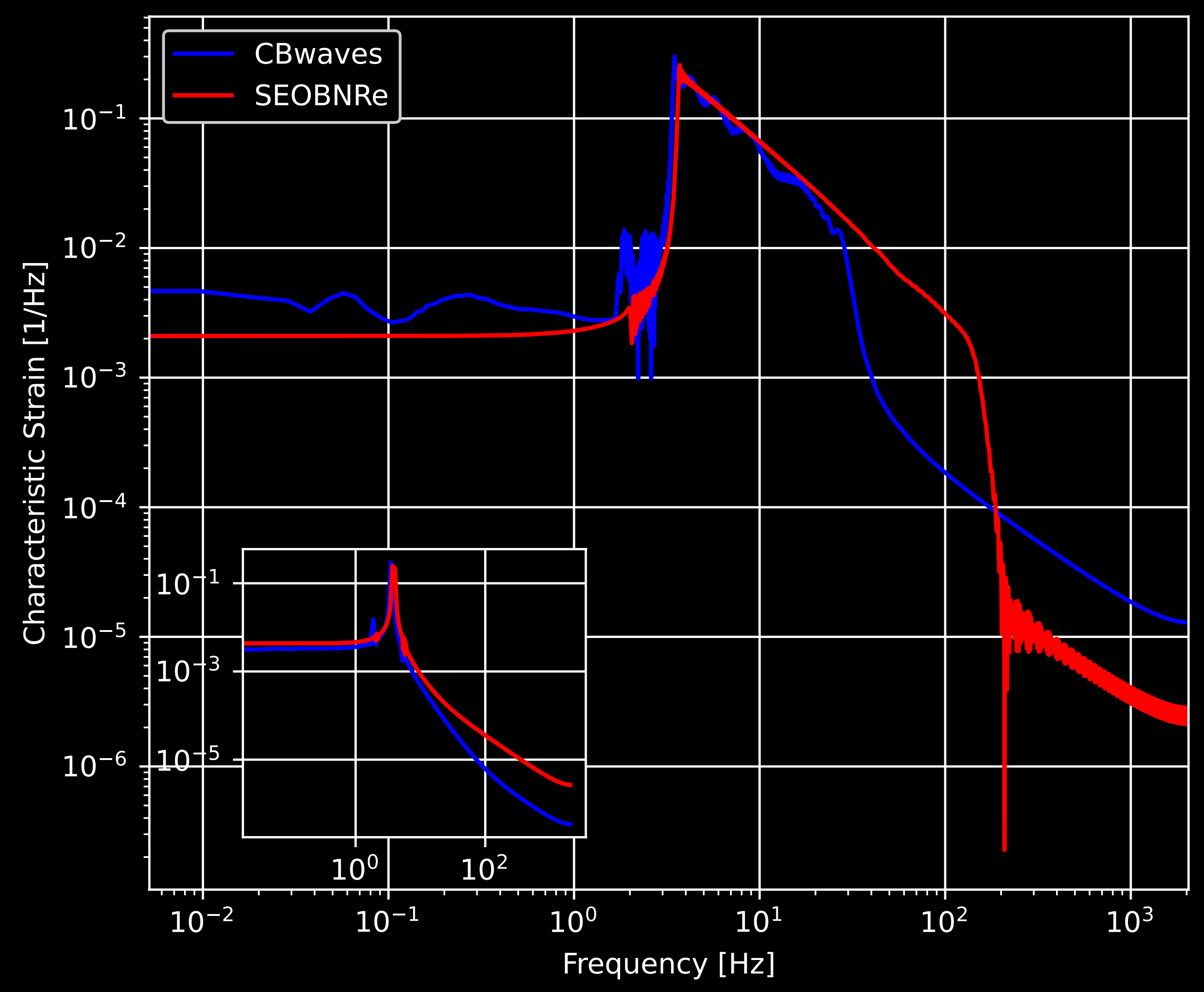

$\chi_1 = 0.6$, ~~aligned~~, $m_2 = 100\ M_\odot$, $m_2 = 10\ M_\odot$

Discussion and Conclusion

- At $1:20$ mass-ratio, the separation computed by both codes is in close agreement
- For configurations with $q < 1/20$ the $6\ \mathrm{M}$ limit reached earlier by $\mathtt{SEBNRE}$
- For configurations with $q > 1/20$ the $6\ \mathrm{M}$ limit reached earlier by $\mathtt{CBWaves}$
- Made detailed contour maps for the mismatch (or unfaithfulness) of various spin configurations
- As the mass-ratio is closing $1:10$, the mismatch between the two models grows larger
- A similar behavior is exhibited toward larger total masses with spins, but irrespective of the spin alignment
- the spins did not retain the initial alignment set in CBwaves
- However, the effects of the spin are unnoticeable on the aligned waveforms

Acknowledgment

- Deeply grateful to **WSCLab.** for computational resources provided
- This work was made in collaboration with **Dániel Barta**
- Thanks for the insight and pieces of advice given by **László Á. Gergely**

Thanks for your attention!

Questions